Sasol Advanced Fuels Laboratory

UNIVERSITY OF CAPE TOWN

Flame Propagation Model for the CFR Engine under Knocking and Non-Knocking Conditions

Author:

Ting-Pang Hsiao

Supervised by:

Mr. André Swarts

A dissertation submitted to the
Department of Mechanical Engineering, University of Cape Town,
in partial fulfilment of the requirements for the degree of
Master of Science in Engineering

Cape Town, South Africa
31 March 2006

Declaration

1. Plagiarism is the illegal use of another's work and pretending that it's one's own.

2. I have used the Harvard convention for citation and referencing. Each significant contribution to, and quotation in, this project from the work(s) of other people has been attributed, and has been cited and referenced.

3. This project is my own work.

4. I have not allowed, and will not allow anyone to copy my work with the intention of passing it off as his or her own work.

Signature Signed by candidate

Date 30/03/2006

Acknowledgement

I am most grateful to my supervisor, Mr. André Swarts, for his guidance and insightful suggestions throughout the course of this project, as well as the very helpful lectures on engine thermodynamics.

This project was funded by Sasol, and the support is gratefully acknowledged.

I would like to thank Dr. Andy Yates for his lectures on engine knowledge and Mr. Carl Viljoen for his lectures on fuel chemistry and properties.

Finally, I would like to thank Mr. Ryan Cox for providing knowledge on CFD modelling and developing the CFD model that is relevant to this project.

Abstract

Engine knock is one of the factors that limit the design of spark-ignition (SI) engines. It is caused by the auto-ignition of the end-gas during combustion and can lead to severe engine damage and failure. Octane number indicates the ability of a fuel to resist auto-ignition in a SI engine and forms part of the gasoline fuel specification. Burn duration of normal combustion is an important parameter during fuel octane measurement and is often equated to the turbulent flame speed of the fuel. The objective of this project is to develop a combustion model using the turbulent flame propagation concept that can be used to study the influence of the underlying flame speed behaviour during combustion. The model was used to investigate the combustion in the CFR engine (the engine used to measure fuel octane number) since it was found previously that the pressure development, and by implication combustion, differs from that found in production engines.

Two flame shape assumptions were found to best describe the combustion event: reversed cylindrical flame and side propagating flame. The model was applied to previously measured data and used to compare the combustion of liquid and gaseous fuels, as well as the fuel performance under different test conditions such as RON, MON and different air-fuel ratios.

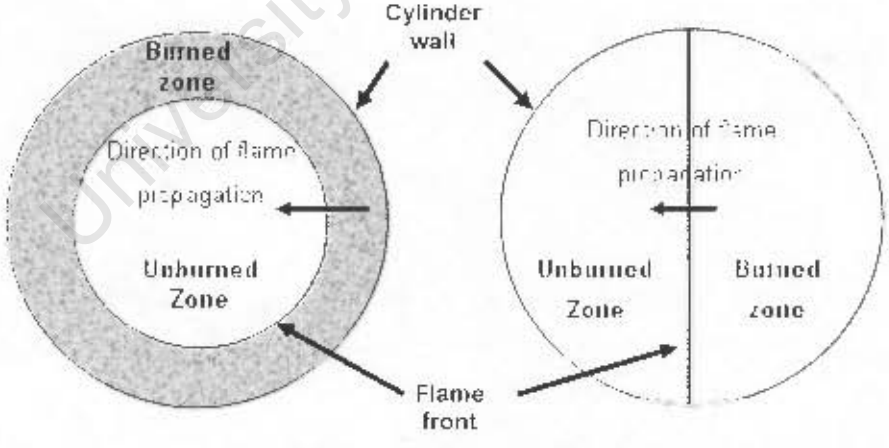

Reversed cylindrical flame (left) and side propagating flame (right)

The influence of thermal boundary layer (TBL) was studied as a possible explanation of the observed pressure development during knocking engine operation in the CFR engine. This pressure development was characterised by the presence of the knock-point where a change

in the rate of combustion was observed after the knock-point. It was hypothesized that the unique development features may be due to an interaction between the auto-ignition and the TBL, but no consistent correlation was found.

The flame propagation model showed good approximation of the actual combustion data prior to the knock-point and was robust and stable. The design of the CFR engine with low compression ratio and side mounted spark plug is the main reason for the post knock-point pressure development, as the design causes localised unburned mixture auto-ignites in a relatively large volume and is similar to HCCI combustion in which auto-ignition combustion occurs without a flame front.

It was recommended that the combustion model can be further modified for better accuracy by considering complex flame shapes. Predictive auto-ignition model can also be included in the flame propagation for more detailed analysis. More fuel tests can be performed for more information on the fuel behaviour. A detailed computational fluid dynamic model can also be considered to simulate the combustion event.

Table of Contents

List of Tables

List of Figures

Nomenclature

CA	-	Crank Angle
CAD	-	Crank Angle Degree
CFD	-	Computational Fluid Dynamic
CFR	-	Cooperative Fuel Research
CR	-	Compression Ratio
EEOC	-	Estimated End of Combustion
EVO	-	Exhaust Valve Opening
TFF	-	Flame Factor
HCCI	-	Homogenous Charged Compression Ignition
KI	-	Knock Intensity
IVC	-	Inlet Valve Closure
IVO	-	Inlet Valve Opening
MFB	-	Mass Fraction Burned
MFU	-	Mass Fraction Unburned
MON	-	Motor Octane Number
ON	-	Octane Number
PRF	-	Primary Reference Fuel
RON	-	Research Octane Number
SA	-	Spark Advance
SI	-	Spark Ignition
TBL	-	Thermal Boundary Layer
TDC	-	Top Dead Centre
TRG	-	Trapped Residual Gas

1. Introduction

1.1 Project Background

Engine knock has been one of the biggest problems associated with *spark-ignition* (SI) engines. Knock in the SI engine is a phenomenon that is caused by the auto-ignition of the end-gas during combustion. It can lead to very severe engine damage and has become a limiting criterion in engine design and engine performance. There are many factors associated with the auto-ignition of the end-gas, such as pressure, temperature, end-gas composition and time. *Octane number* (ON) indicates the ability of a fuel to resist auto-ignition during combustion where a higher ON means a lower chance that the fuel will auto-ignite before the end of combustion. The fuel ON is obtained in fuel octane measurements involving a single cylinder, variable compression ratio *Cooperative Fuel Research* (CFR) engine. As the results of these tests, the fuel is generally rated with both a *research octane number* (RON) and a *motor octane number* (MON) which are obtained under different conditions as prescribed by the ASTM (ASTM, 2001a,b).

Burn duration of gasoline in SI engines is an important parameter during octane measurements. A combination of fuel combustion and piston motion is the main cause of in-cylinder pressure and temperature development. Variation in fuel burn duration results in different end-gas conditions. For example, shorter burn duration means that fuel is consumed in shorter time, leading to a more rapid energy release rate and results in more severe pressure and temperature rise. Under this condition, the fuel would more likely to auto-ignite and inevitably obtain a lower octane rating from the octane measurements.

Fuel burn duration is known to be affected by fuel composition, engine design and engine operating conditions (Heywood, 1988 and Taylor and Taylor, 1962). It is normally studied with the fuel flame speed and the relationship between the two is very closely linked. In-cylinder flame speed can be classified into two categories: laminar flame speed and turbulent flame speed. Heywood (1988) describes that laminar flame speed is mainly affected by the chemical properties of the fuel and the engine operating conditions such as pressure, temperature and air/fuel ratio. However, as the engine speed increases, the time available for combustion becomes relatively shorter. Turbulent flame speed caused by the inlet air

motion and the piston movement then becomes the more significant factor during combustion.

In commercial engines knock can be identified by the very extreme pressure rise and followed by pressure oscillations, and it is generally agreed that the point of knock is where the rapid pressure rise begins. This behaviour is somehow different in the CFR engine where the initial pressure rise and the pressure oscillation are more "gentle" when compared with commercial engines as shown by Arrigoni et al. (1974). Konig and Sheppard (1990) have also pointed out this phenomenon in their research as they observed a 'significant, but not particularly rapid, rate of pressure rise' behaviour towards the end of combustion. They have also concluded that although knock is caused by the auto-ignition of the end-gas, auto-ignition of the end-gas may not always result in knock. The research group in the SASOL Advanced Fuel Laboratory later discovered that the knock traces observed from the CFR engine may not be the result of an actual knock phenomenon (Swarts et al., 2004, 2005).

1.2 Project Objectives

The objectives of this report are to:

a) Develop a combustion model adopting the flame propagation concept. With the combustion model, study the fuel behaviour in the CFR engine using the pressure data obtained from the CFR engine and extract information from those pressure data. Studies would be carried out for a range of fuels, including both liquid and gaseous fuels at different speeds applicable to RON and MON conditions.

b) Investigate the unique knocking behaviour that occurs in the CFR engines which differs from commercial engines, and find reasons and explanations for this behaviour. Furthermore, investigate on any possible connection between this behaviour and the results from octane testing.

1.3 Plans of Development

Chapter 2 aims to give a background understanding on this project. It presents the octane test conditions and the design of the CFR engine, as well as information on the flame and pressure developments of the SI engines. It is followed by literature on some of the key factors that are relevant to combustion model development.

Chapter 3 focuses on the development of the flame propagation model. Basic engine combustion thermodynamics and chemistry are included in this chapter and the different models used are presented. These include the flame propagation model and a multidimensional engine inlet model that can used to predict the initial conditions for combustion models.

Chapter 4 presents the existing data obtained from the CFR engine and the results on the flame propagation model. The model is applied to both knocking and non-knocking conditions. Comparisons and discussions are made between experimental and simulated results. Based on these results, conclusions were drawn and recommendations are made in Chapter 5.

2. Literature Review

2.1 Octane Test Conditions

There are several octane rating methods and the two most commonly known are RON and MON methods. Both methods are carried out in the CFR engine under conditions prescribed by ASTM. In the MON method the operating conditions are configured to be closer to road conditions, such as higher engine speed and inlet temperature. During the octane test, the test fuel is used to operate the engine and the *compression ratio* (CR) is adjusted so that standard *knock intensity* (KI) is reached. A blend of fuel which is referred to as *primary reference fuel* (PRF) is then used to operate on the engine under the same conditions to produce the same KI. PRF is a fuel made up by blending iso-octane and n-heptane, and it is numbered according to the volume ratio of the two fuels. For example a blend of 90% iso-octane and 10% n-heptane by volume will be known as PRF90. RON and MON rating of the test fuels are determined by the PRF number that is used to produce the same KI under the same test condition and CR. A summary of the operating conditions of RON and MON methods are listed below:

Table 2-1: Operating conditions for the RON and MON methods

	Research method	Motor method
Inlet Temperature	52°C (125°F)	149°C (300°F)
Inlet Pressure	Atmospheric pressure (1 Bar)	
Engine Speed	600 rpm	900 rpm
Spark Advance	13° BTDC	19 -26° BTDC (varied with CR)
Compression Ratio	Adjusted for standard knock intensity	

2.2 CFR Engine Design

CFR engine is a four-stroke single cylinder engine that is used as the standard test engine for determining the ON of different fuels. It is carburetted and has a fixed stroke which gives

constant displacement volume. The position of the cylinder head can be altered to give different clearance volume and this allows the CFR engine to have variable CR. The cylinder head is flat, as well as the top of the piston and this forms a near-cylindrical combustion chamber. The spark plug is mounted on the side of the combustion chamber and it results in a longer flame path by comparison since the flame front has to travel across the whole combustion chamber. The inlet valve is fitted with an 180° shroud and the shroud forces the inlet mixture to go through one side of the valve. The inlet valve is fitted in a way that the inlet mixture is directed along the cylinder wall and away from the spark plug. The CFR engine parameters and a sketch showing the CFR engine design are shown below:

Table 2-2: CFR engine parameters

Parameter	Value
Cylinder Bore	82.55 mm
Stroke	114.3 mm
Compression Ratio	Variable
Inlet Valve Closure (IVC)	146° BTDC
Exhaust Valve Open (EVO)	140° ATDC
Valve Diameter	35 mm
Max Valve Lift	8mm

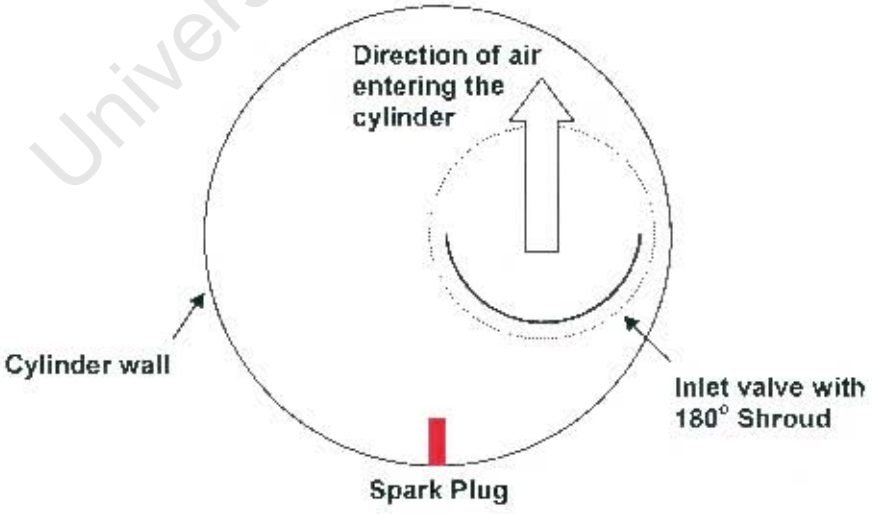

Figure 2-1: A simple sketch illustrating the spark plug and shroud position in the CFR engine

2.3 Knock in SI Engines

2.3.1 General

Knock is the most concerned abnormal combustion phenomenon in SI engine, and its name came from the noise that results from the auto-ignition of a portion of the fuel (Heywood, 1988). When the flame propagates across the combustion chamber, it compresses the unburned mixture in front of the flame front (end-gas) and causes the end-gas pressure and temperature to increase. Under appropriate conditions, the end-gas may auto-ignite even though it has not yet been consumed by the propagating flame front. When it happens, the end-gas undergoes very rapid combustion and energy release, causing high frequency pressure oscillations inside the combustion chamber and produces a knocking noise (Heywood, 1988).

End-gas auto-ignition in the SI engine is highly dependant on the pressure and temperature history, and it requires a certain amount of exposure time under the pressure and temperature influence for auto-ignition to occur. There are a few factors that are relevant to these conditions:

- Inlet pressure: increasing the inlet pressure increases the peak pressure during combustion, and this increases the probability of knock.

- Inlet temperature: increasing the inlet temperature will increase end-gas temperature, which increases the possibility of knock.

- Compression ratio: compression ratio has a significant effect on the end-gas pressure and temperature. Increasing the CR will increase both temperature and pressure, and it will significantly increase the probability of knock.

- Combustion chamber design: this affects combustion in two ways, the flame path and turbulence inside the combustion chamber. The flame path is mainly determined by the position of the spark plug and affects the distance that the flame has to travel during combustion. This further affects the end-gas exposure time under high pressure and temperature. Turbulence within the combustion chamber can be changed by altering the shape of the combustion chamber, such as adding squish zone or forcing swirls inside

the combustion chamber. Research (Fujimoto et al., 2002) has shown that by adding a squish area inside the combustion chamber, it enhances the combustion and increases power output of the engine.

- Spark advance: spark advance is most commonly used to control knock in SI engines, by retarding the spark advance, the peak pressure and temperature is reduced, which decrease the chance of knock and vice versa.

It is important however, to understand that although knock is caused by auto-ignition of the end-gas, auto-ignition will not always lead to knock (Konig and Sheppard, 1990). Shown in the following is a typical knocking pressure trace that would be seen on a commercial engine. It is very clearly shown in the graph, with regard to the very rapid pressure rise at the point of knock and the pressure oscillation that follows.

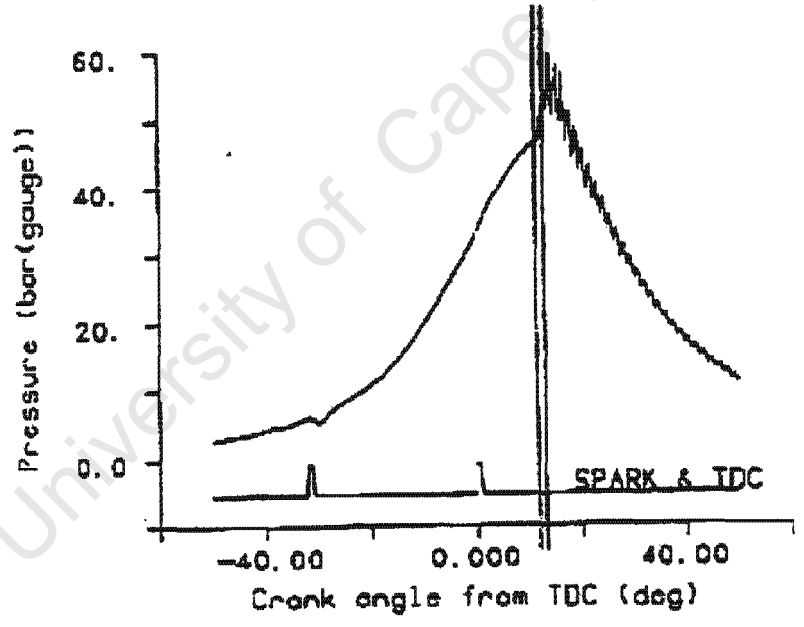

Figure 2-2: A typical knock pressure trace in commercial engines (Konig and Sheppard, 1990)

2.3.2 CFR pressure development

Knocking inside the CFR engine is characteristically different to what happens in the commercial engine. Arrigoni et al. (1974) reported an untypical pressure development that occurred in the CFR engine. They observed that knock in CFR engines takes place with an increase in pressure often higher than that in the case of commercial engines. This pressure

rise affects the pressure oscillations that follow, and the pressure oscillations are generally smaller than those that occur in commercial engines. Broeze (Unknown) also referred to the CFR knocking condition in his research work and showed a change in combustion pressure traces. This phenomenon was also observed by Maly and Ziegler (1982) in their research work on the L-head engines. The following Figure was used by Arrigoni et al. (1974) to illustrate the phenomenon observed in the CFR engines.

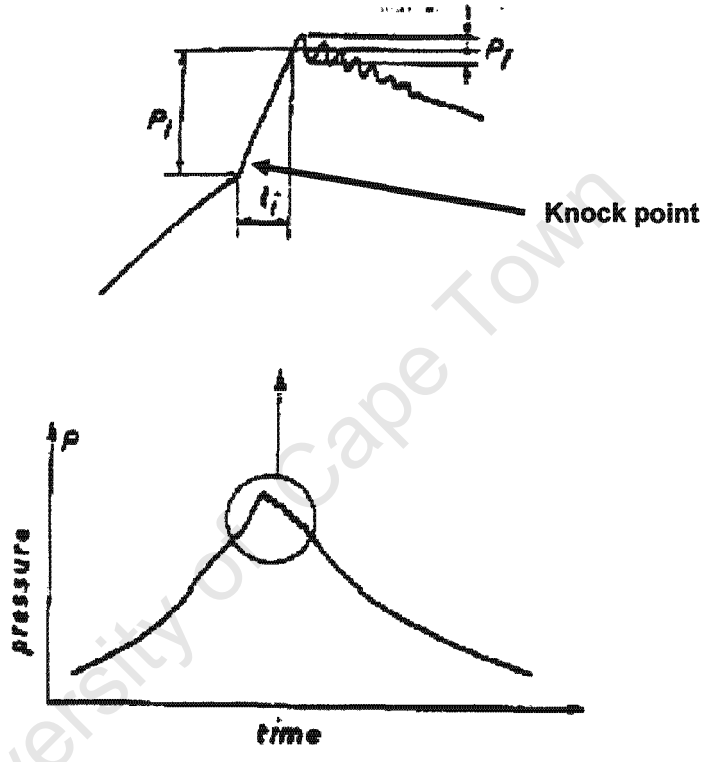

Figure 2-3: Pressure trace showing the knock behaviour in a CFR engine (Arrigoni et al., 1974)

The research group in the Sasol Advanced Fuels Laboratory at the University of Cape Town has done tests in the CFR engine using a range of PRF with RON of 40 to 100. The point where this initial change of slope occurred in the pressure trace was termed the "knock-point". Results showed that the position of the knock-point changes with different RON and the MFB at the knock-point was not consistent for the standard KI (Swarts et al., 2004, 2005). Uncertain about the origins of this phenomenon, it was subsequently concluded to be progressive auto-ignition (developing detonation) (Swarts, 2006).

Pressure traces that are very similar to the above Figure were observed in *homogeneous charged compression ignition* (HCCI) engines, where HCCI by definition means 'lean auto-ignition combustion of a fuel without a flame front'. Research work by Flowers et al. (2000)

and the later work by Aceves et al. (2001) both presented HCCI combustion pressure traces that are very similar in appearance to the CFR knocking pressure traces.

The following Figure was taken from Flowers et al. (2000) to illustrate the HCCI combustion pressure traces.

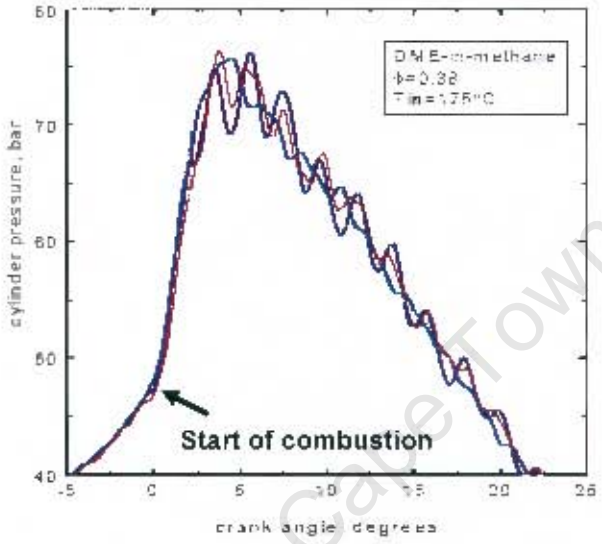

Figure 2-4: HCCI combustion pressure traces (Flowers et al., 2000)

Combustion in HCCI engines can be recognized by the sudden change of the pressure trace slope and followed by near-linear rapid pressure rise as well as pressure oscillation. It is clear that the start of HCCI combustion pressure traces is very similar to the knock pressure trace observed in the CFR engine data. The main difference between the two pressure traces is that HCCI combustion pressure traces cover the full MFB region and consumes all the fuel mixture. In the case of the CFR engine, the combustion pressure trace consists of two stages: pressure increase due to normal flame propagation combustion and auto-ignition of the end-gas not consumed by the flame front. The HCCI combustion pressure trace showed similar behaviour with the portion of the pressure development that is caused by auto-ignition.

2.4 Mass Fraction Burned

Mass fraction burned (MFB) represents the fraction of the fuel/air mixture that is consumed during combustion. It is a measure of the fraction of fuel energy release over the total energy release during combustion. It also shows the rate of combustion which contributes to the cylinder pressure and temperature development. MFB is very useful for characterising combustion behaviour since cycle-to-cycle variations causes pressure traces to vary. During combustion, the mixture is divided into the burned gas and the unburned gas, separated by the propagating flame front. Energy was released by the mixture that was consumed by the flame front and caused the burned zone to reach a much higher temperature than the unburned zone. This results in a lower density within the burned zone. Since it is still impossible to measure MFB during combustion, MFB must be inferred from measured pressure data.

There are alternative ways of obtaining MFB during combustion. It is achieved by analysing the results that are available during combustion. A model developed by Rassweiler and Withrow (1938) was found to give the best results in predicting MFB after comparing with a few other methods by Brunt and Emtage (1997).

The Rassweiler and Withrow method proposed that MFB can be determined as a function of pressure rise during combustion; the Equation is given as follows:

$$MFB_{\theta} = \frac{\sum_{i=ign}^{i=\theta} \Delta P_{c,i}}{\sum_{i=ign}^{i=EEOC} \Delta P_{c,i}} \qquad (2.1)$$

where

MFB_{θ} = mass fraction burned at crank angle θ,

$\Delta P_{c,i}$ = corrected pressure rise due to combustion,

i = integer crank angle location,

ign = crank angle position at which the spark is initiated,

EEOC = crank angle position at the estimated end of combustion.

The corrected pressure rise due to combustion is calculated from the difference between incremental measured pressure rise and the pressure rise corresponding to a polytropic compression/expansion process, referenced to the cylinder volume at *top dead centre* (TDC).

$$\Delta P_{c,i} = [P_i - (\frac{V_{i-1}}{V_i})^n P_{i-1}] \cdot (\frac{V_{i-1}}{V_r}) \qquad (2.2)$$

where

n = assumed polytropic coefficient,

V_i = cylinder volume at crank angle i,

V_r = referenced cylinder volume at TDC.

In this model, EEOC is determined from the *crank angle* (CA) position where the value of $pV^{1.15}$ reaches a maximum.

2.5 Flame Speed

In ideal standard fuel-air cycles, combustion is normally assumed to occur instantaneously inside the combustion chamber to simplify calculation. However, combustions in the engines are actually more progressive than instantaneous. Research (Lee and Lee, 2003) has shown that during combustion, the burned and unburned zones are separated by a distinct flame front. As the gas mixture is consumed by the flame, the burned mixture expands and pushes the flame front into the unburned mixture. The propagating flame compresses the unburned mixture and causes its pressure and temperature to increase which could later lead to auto-ignition.

The speed at which the flame propagates into the unburned mixture is referred to as the flame speed. Flame speed in SI engines is a combination of two parts that are related: laminar flame speed and turbulent flame speed, and it is a fundamental parameter that influences the engine performance (Hacohen et al., 1994).

Laminar flame speed (S_L) was shown to be a function of fuel composition, temperature and pressure in the research by Ryan and Lestz (1980). The researchers suggested that S_L can be expressed using the following Equation:

$$S_L = b_1 P_u^{b_2} \exp\left(\frac{-b_3}{Tu}\right) \tag{2.3}$$

where P_u and T_u are the unburned pressure and temperature respectively, and b_1, b_2 and b_3 are different constants for different fuels and equivalence ratios.

Heywood (1988) also suggested that S_L can be expressed as follows:

$$S_L = S_{L,0}\left(\frac{T_u}{T_0}\right)^{\alpha}\left(\frac{p}{p_0}\right)^{\beta} \tag{2.4}$$

where T_0 = 298 K and p_0 = 1 atm are the reference temperature and pressure. $S_{L,0}$, α, and β are constants for a given fuel, equivalence ratio, and burned gas diluents fraction.

Laminar flame speed for a typical SI engine fuel which generally operates at stoichiometric conditions is about 30-40 cm/s. The magnitude of the laminar flame speed has very little effect on the overall combustion in SI engines which only allow a few milliseconds for a complete combustion, and turbulent combustion thus has a more significant effect. Turbulent flame speed is more complicated the laminar flame speed, and it is affected by the expansion of the burned gas and piston motion (Lee et al., 1998). Other researches (Lee and Lee, 2003; Bradley et al. 2003; Kumar and Watson, 1988) have also shown that turbulence within the combustion chamber breaks up the flame front, exposing a larger contact area between the burned and unburned gases. It results in enhanced heat transfer between the mixtures, hence increase the flame speed.

Kuehl (1962) suggested that is possible to approximate flame speed by multiplying S_L by a flame factor 'ff', such that:

$$S_T = ff \times S_L \tag{2.5}$$

The value for ff is either calculated or obtained experimentally.

Keck (1982) also suggested that S_T can be expressed as a combination of the laminar burning speed and the effect of turbulence. This leads to the following expression:

$$S_T \approx u_T + S_L \tag{2.6}$$

where u_t is the characteristic velocity due to turbulent convection and is calculated from gas velocity and density, which can be obtained using gas dynamics.

2.6 Combustion Model

2.6.1 Flame shape

Two-zone combustion models were often used in various studies (Benson et al., 1975; Fan and Reitz, 2001). These models uses thermodynamic and combustion chemistry equations to solve for energy balance during combustion. Planar, hemispherical or spherical flame shapes were often used for calculation of the flame front position in these models:

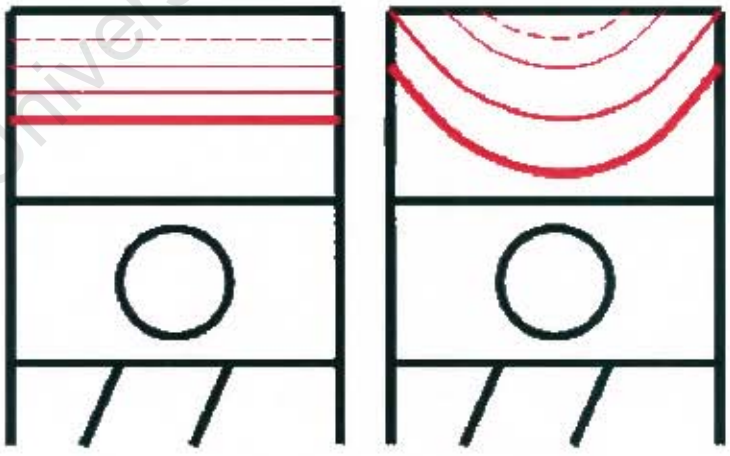

Figure 2-5: Flame shape assumptions used in literature

With the use of flame speed formulation discussed in section 2.5, the flame shape assumption allows the calculation of the burned gas volume. The calculated volume is then required to be converted to the burned gas mass. Mass of the burned gas can be calculated

from the volume and the density, which is a function of gas properties, combustion pressure and temperature. MFB can then be calculated and used to compare with the engine data obtained from the engine experiments to validate the flame shape assumption.

2.6.2 Functional descriptor of MFB

A functional descriptor of the data obtained using the Rassweiler and Withrow model, discussed in section 2.4, provides a convenient empirical model of the MFB. The most commonly used is the Wiebe function (Heywood, 1988) and it can describe the shape or behaviour of the MFB by choosing appropriate parameters:

$$x_\theta = 1 - \exp\left[-a\left(\frac{\theta-\theta_0}{\Delta\theta}\right)\right]^{m+1} \tag{2.7}$$

where

x_θ = MFB calculated at a giving crank angle θ

θ = specific crank angle degree at point of calculation,

θ_0 = start of combustion,

$\Delta\theta$ = total combustion duration,

a and m are parameters used to adjust the shape of the curve.

An alternative model was proposed by Oppenheim and Kuhl (1998) and is referred to as the fuel life function. Formulation of the function is as follows:

$$x_\theta = \frac{\exp\left[-\alpha(1-\Theta)^\beta\right] - \exp(-\alpha)}{1-\exp(-\alpha)} \tag{2.8}$$

And

$$\Theta = \left(\frac{\theta-\theta_0}{\Delta\theta}\right) \tag{2.9}$$

This function is also specified by two parameters, α and β, which are used to characterise the behaviour of the function.

3. Combustion Model

3.1 Engine Thermodynamic and Combustion Chemistry

The ideal four-stroke engine cycle begins with the compression of the fuel/air mixture, which increases the pressure and temperature inside the combustion chamber. This mixture is then ignited by the spark and combustion of the mixture forces the piston to expand. Combustion products leave the cylinder at the end of expansion and fresh mixture is drawn in again to start another cycle. Overall energy balance is remained during the combustion process according to the first law of thermal dynamics (Cengel and Boles, 2002).

The idealised combustion of hydro-carbon of the fuel/air mixture under stoichiometric condition reactions can be described by the following general reaction (Sonntag et al. 1998; Heywood, 1988) where the terms will be referred to as reactants and products.

$$C_xH_y + (x + \frac{y}{4})O_2 + zN_2 \longrightarrow xCO_2 + \frac{y}{2}H_2O + zN_2 \qquad (3.1)$$

Reactants **Products**

N_2 is assumed to be inert and does not participate in any reaction. Both reactants and products are treated as ideal gases and obey the ideal gas law (Heywood, 1988). With the high pressure and temperature caused by the combustion of fuels, a number of equilibrium reactions, dissociation of the CO_2 and the water-gas shift reaction will also occur. This gives rise to the function of CO and H_2:

$$CO + \frac{1}{2}O_2 \longleftrightarrow CO_2 \qquad (3.2)$$

$$CO_2 + H_2 \longleftrightarrow CO + H_2O \qquad (3.3)$$

The rates of the two reactions are governed by thermodynamic equilibrium and the partial pressure of individual gas components as described by Dalton's law (Cengel and Boles,

2002). Details with regard to the thermodynamics and the chemical equilibrium can be found in general thermodynamic textbooks.

At the exhaust stroke, waste gas/product with the volume approximately equal to the displacement volume of the engine is ejected out of the cylinder. Gas within the clearance volume remains inside the cylinder and is generally referred to as the *trapped residual gas* (TRG). TRG is considered to be a part of the reactants for the new cycle. Considering the effect of TRG, equations (3.1) to (3.3) can be combined and modified, which forms the following Equation. The molar coefficients of terms are not included in the Equation since they are dependant on the operating conditions and fuels.

$$C_X H_Y + O_2 + N_2 + CO_2 + H_2O + CO + H_2 \longrightarrow CO_2 + H_2O + O_2 + N_2 + CO + H_2 \tag{3.4}$$

3.2 Two Zone Model

3.2.1 Functional descriptor

Engine models are developed in order to simulate the combustion event to compare with real data and a two zone model is suited for this application. A two zone combustion model consists of the burned zone and the unburned zone, separated by the thin flame front. Wiebe function is commonly used in computer models to represent MFB (Heywood, 1988); it is a mathematically formulated heat release model that is able to produce curves similar to MFB curves. Formulation of the Wiebe function is as follow:

$$x_\theta = 1 - \exp\left[-a\left(\frac{\theta - \theta_0}{\Delta\theta}\right)\right]^{m+1} \tag{3.5}$$

where

x_θ = MFB calculated at a giving crank angle θ

θ = specific crank angle degree at point of calculation,

θ_0 = start of combustion,

$\Delta\theta$ = total combustion duration,

a and m are parameters used to adjust the shape of the curve.

In order to produce simulated results that are very similar to real data, the MFB behaviour is used to compare the theoretical and actual results. The use of such heat release model for the purpose of this project is however very limited. This is because the Wiebe function can only produce a symmetrical curve to represent MFB. Normal combustion in the SI engine can be identified in three stages:

- ignition delay and early flame development,
- main combustion event with rapid combustion of the mixture,
- combustion cool-down.

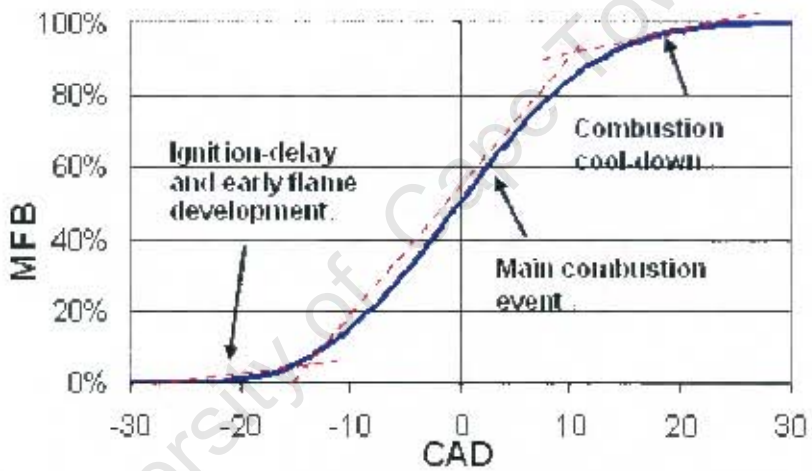

Figure 3-1: The three stages of a normal combustion in a SI engine

At all three stages the rates of fuel consumption differ, and observations were also made between different fuel types and engine operating conditions. Symmetrical curves produced with the Wiebe function could not adequately estimate combustion in real engines and hence was not used as an input for the simulation. Comparison of the two results is illustrated in the following Figure. It should be noted for the difference between the two sets of data, as well as the clear difference in the start and end of combustion on the CFR engine data.

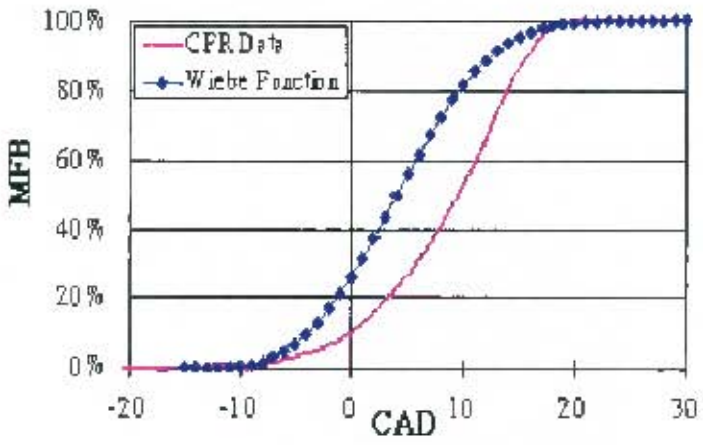

Figure 3-2: Comparison between CFR engine data and the curve produced using the Wiebe function

Other heat release models such as the fuel life function were also proved not to be adequate to represent the fuel MFB characteristics over the entire combustion event (Swarts et al., 2004). Since the use of the heat release model was not suited for the applications of this project, a different approach was required. In order to analyse the fuel behaviour, an empirical computer model was required to physically relate theoretical simulations with experimental results.

3.2.2 Flame propagation model

A two zone flame propagation model was developed for this project, adapting the basic engine thermodynamics. The shape of the flame front is often complicated and in this model it was assumed that the flame front is infinitely thin and there is no folding or wrinkle in between the two zones. This assumption was combined with the assumption that the burned zone behind the flame front contains no unburned gas. The reactant was assumed to be homogeneous at uniform temperature and the pressure is uniform throughout the cylinder according to Dalton's law. It was also assumed that there is no gap between the piston and the cylinder wall, hence providing no crevice volume to trap fuel and no mass loss during combustion. Flame speed formulation suggested by Heywood (1988) and Kuehl (1962) as discussed earlier in this report was adopted for this model. A simple diagram is used to illustrate this concept:

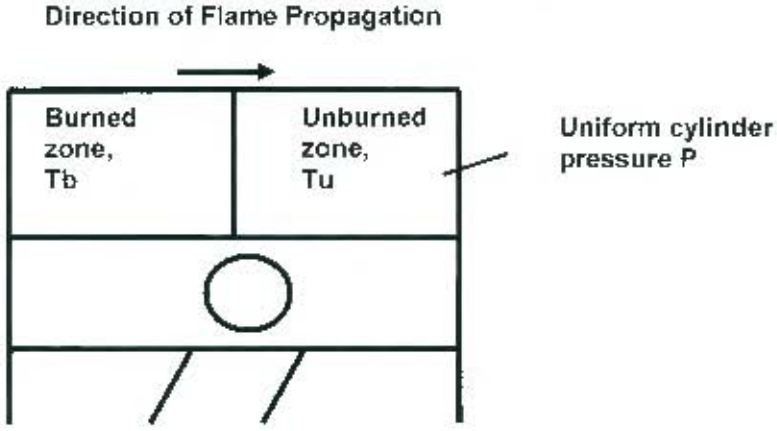

Figure 3-3: Simple illustration of the two zone model concept

The objective of this model was not to simulate the flame propagation behaviour due to complex mathematics but rather to simulate the MFB behaviour in real engines with appropriate flame shape assumptions. Previous studies (Benson et al., 1975; Fan and Reitz, 2001) assumed either a hemispherical or spherical flame front, and these flame shapes did not give good MFB approximation due to very slow early flame development ($V \alpha R^3$) and very short cool-down period as the flame travels into the boundaries. Other flame shapes such as planar flame propagating from cylinder top towards piston head or cylindrical flame shapes were also tested and the results did not show good approximations.

The following Figure shows comparison between the mentioned flame shapes and the actual data. MFB data of propane under the non-knocking RON condition and CR of 7.9 was used for comparison.

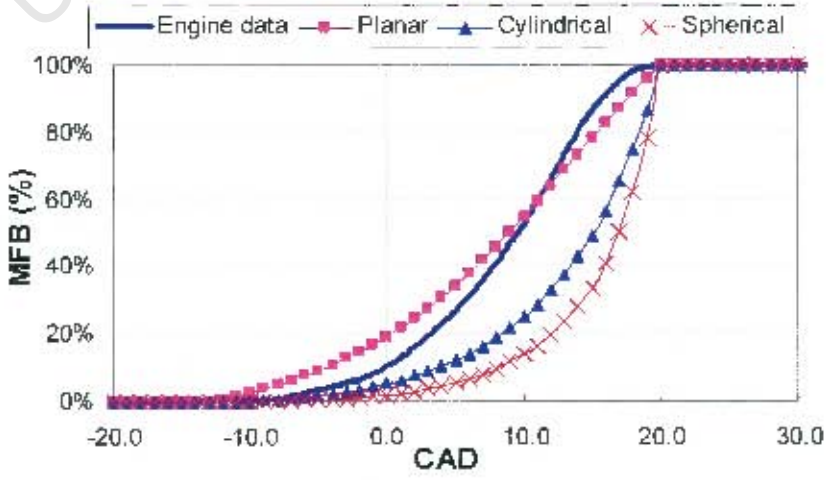

Figure 3-4: Comparison of MFB curve obtained from CFR engine and simulation results

3.3 Three Zone Model

The CFR engine knocking pressure development showed auto-ignition behaviour which is very similar to the particular mode of knocking described by Konig and Sheppard (2000) as developing detonation. Research by Pan and Sheppard (1994) showed that the modes of end-gas auto-ignition are strongly affected by the temperature gradient. Apart from the temperature gradient that is present within the gas mixture, it can also be observed to exist in the *thermal boundary layer* (TBL) near the cylinder walls. This gives rise to the concept that the presence of the TBL may play a role in the knocking behaviour in the CFR engine.

In order to study the effects that TBL has on the CFR knock behaviour; it was required to incorporate the TBL into the engine model. A three zone model developed by Hajireza et al. (1999) was adopted for this purpose. The three zones that were defined in this model are shown as follows:

- Zone I: Burned zone
- Zone II: Unburned zone outside thermal boundary layer
- Zone III: Unburned zone within thermal boundary layer

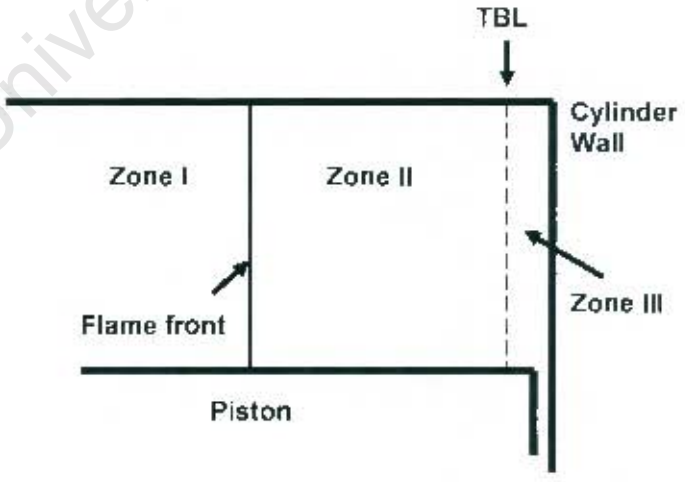

Figure 3-5: Schematic diagram of the three-zone model concept

Thickness of the TBL was calculated based on research by Lyford-Pike and Heywood (1984), which stated that the thickness is dependent on thermal diffusivity and the time needed for the layer to develop. They have also found a correlation between the Reynolds number and the growth of the TBL. The thickness of the TBL is calculated as follows:

$$\delta = 0.6\,\mathrm{Re}^{0.2}\sqrt{at} \tag{3.6}$$

where

δ = thermal boundary layer thickness

a = thermal diffusivity

t = time from TDC

The minimum thickness of the TBL was taken as 0.01mm, and this is to avoid the unrealistic behaviour that may be encountered during calculation.

The Reynold's number (Re) is calculated as:

$$\mathrm{Re} = \frac{\rho v x_0}{\mu} \tag{3.7}$$

where ρ, v, μ are the gas density, velocity and viscosity, and it was assumed that there is a linear relationship between the gas velocity and the piston velocity, such that:

$$v = v_p\left(\frac{x_0}{x}\right) \tag{3.8}$$

where

v = gas velocity

v_p = piston velocity

x = distance between the piston head and the cylinder head

x_0 = distance of calculated location from the cylinder head which gives a average temperature distribution inside the TBL

The value of x_f was taken as 1/3 and this was to obtain an averaged TBL thickness since it is not constant in all sections of the cylinder.

This three-zone model concept was combined with the two-zone model to form a three zone flame propagation model. The same thermodynamic assumptions were used, as well as the same flame shape assumptions.

3.4 Multidimensional Model

3.4.1 Background

Since the CFR engine has an 180° shrouded inlet valve, it is expected to change direction of the inlet air and induce a swirling motion in the cylinder. The placement of the shroud results in only a half of the valve opening area being available for air entrance. Since the volume flow rate and the valve opening time remains the same, the inlet air would be forced to enter the cylinder at a higher speed. It will result in a higher in-cylinder air velocity and have a significant effect on the level of turbulence inside the cylinder. In order to develop the flame propagation model, it was required to find the appropriate flame front shape assumption, as it determines the behaviour of the flame development. Since turbulence was known to affect combustion, more importantly the early flame development, it is important to study the effect of the shroud on the in-cylinder turbulence. Understanding the turbulent air motion inside the cylinder during inlet and even at the point when the spark is ignited would contribute to better assumptions made on the flame shape for the flame propagation model.

A *Computational Fluid Dynamic* (CFD) approach was used to study the behaviour of air flow inside the cylinder during the engine inlet cycle. CFD is the analysis of systems that involve fluid flow and heat transfer (Versteeg, 1995). It uses numerical techniques to simulate these events. The main advantage of the CFD approach is that it is able to simulate certain areas and processes where experimental results are difficult or sometimes impossible to obtain.

The CFD process begins with constructing a 'mesh' of the analysed object, where the object expressed as a combination of individual cells using the finite element technique. Relevant information can be extracted by solving the governing equations within the mesh with an iterative method.

The CFD codes consists of 3 parts: the pre-processor, solver and post processor (Cox, 2004):

a) Pre-Processor

The pre-processor is used to create the geometry of the simulating object and construct the mesh for the object. Other specifications such as boundary and fluid properties are also defined here. The solution becomes more accurate as the number of cells in the mesh increases. However the computational time will also increase as the number of cells increases. This results in the requirement for the balance between the accuracy requirements and the computational requirements.

b) Solver

The solver performs calculation on the mesh that is produced by the pre-processor. The user must define certain criteria before the calculation begins. That is, the initial conditions, as well as the results that are relevant and need to be extracted, such as pressure, temperature, etc. While solving unsteady events such as the engine, the model is also divided into time steps where each time step is solved as a steady state event. In this study, Fluent (1998) (the commercial CFD package used at UCT) is used to perform these calculations. The following picture shows one of the CFD calculation logic diagram:

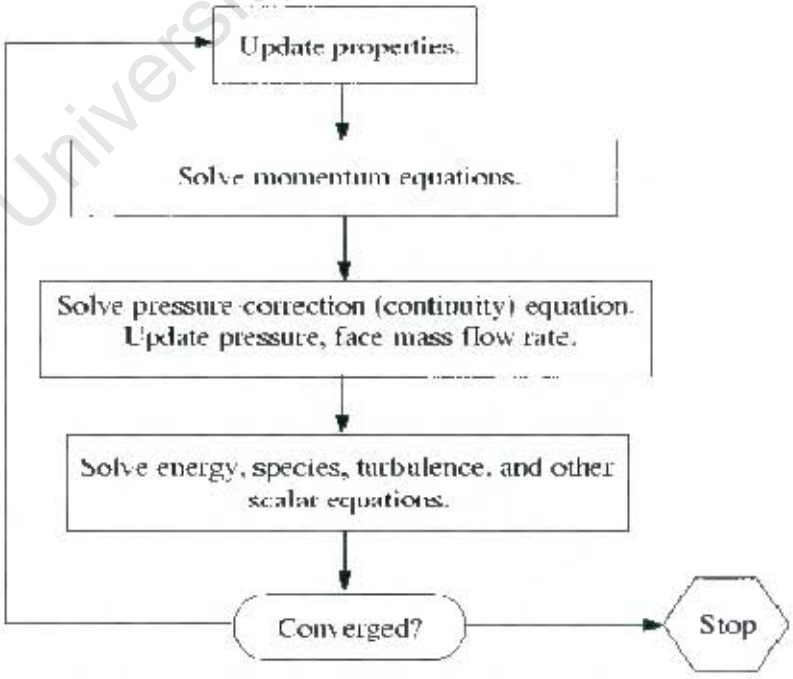

Figure 3-6: Logic diagram showing the process segregated solver (Fluent, 1998)

c) *Post Processor*

The post processor contains the visualisation tools that can present the results in an easy to understand format. It is capable of producing results such as graphs, vector and contour display and is mainly used as an aid to the users' understanding of the results.

3.4.2 Model description

An existing 3-dimensional CFD simulated engine inlet model (Cox, 2004, 2005) was adopted to study the engine inlet process. It was originally developed to simulate the SI engine and study the in-cylinder fuel behaviour. A combination of meshes was used in this model to cater for the moving inlet valve and the moving piston. The following Figure shows the sectional view of the model.

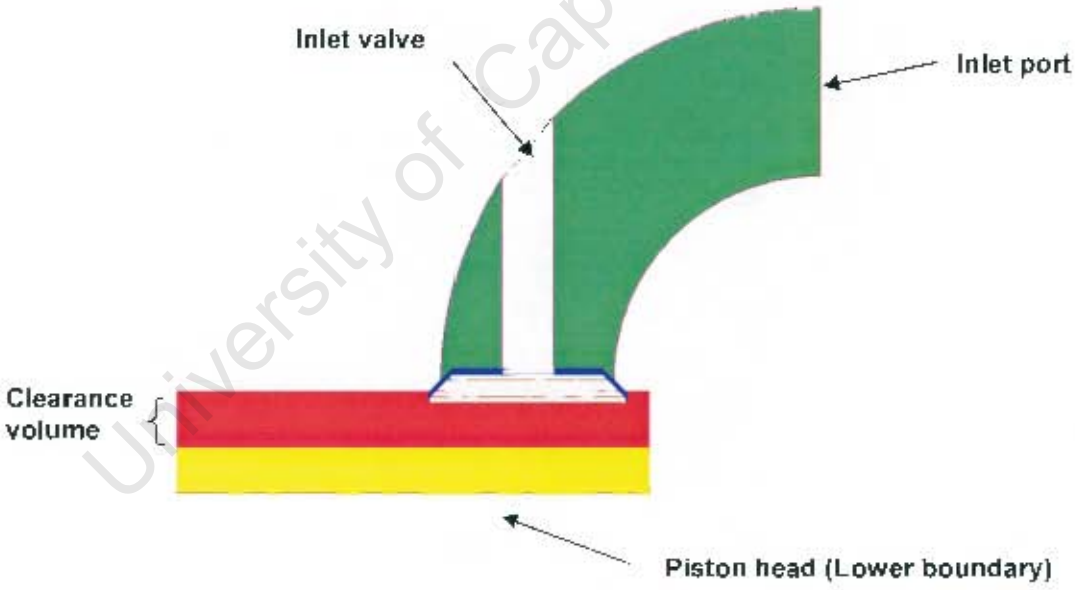

Figure 3-7: Sectional view of the CFD model where each colour represents a different mesh

This model was formed with 4 zones that are connected and 2 types of mesh style. The area with green colour represents the inlet port and is the source of the inlet air. Unstructured mesh is used to form the inlet port to reduce computational time and because this area does not require detailed analysis. The inlet valve is not a zone in the model since there is no fluid at present; therefore it is treated as a moving boundary. The blue area between the inlet port and the valve is referred to as layer. This area is formed by fine structured mesh that can be

easily resized to cater for the valve movement. This is a technique used to cater for the moving inlet valve. The red area is the clearance volume of the cylinder. Unstructured mesh is used in this area. The yellow area is where the piston moves and a structured mesh is used in this area for the same reason as for the layer which caters for moving parts. The piston is also not treated as a zone since there is no fluid flow. The piston is replaced by a moving lower boundary that represents the piston head.

This model was modified to suit the CFR engine operating conditions and a shrouded valve was included. The following mesh shows the final CFD model and the mesh formation.

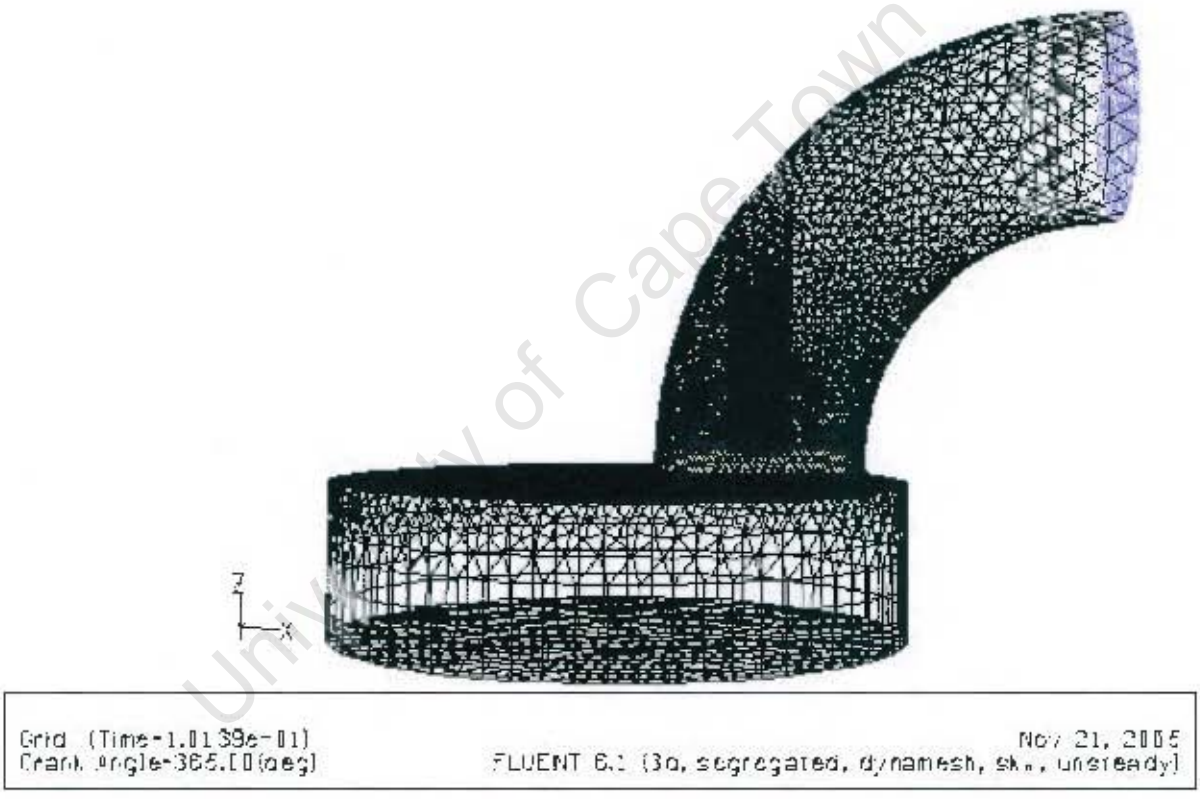

Figure 3-8: 3D Mesh created for CFD analysis on the CFR engine with shrouded valve

4. Results and Discussions

4.1 Experimental Data

A range of fuels were tested in the CFR engine under RON and MON conditions for a range of CR's and pressure traces were recorded. It is almost impossible to analyse all of the results as there are hundreds of pressure traces for each fuel under each test condition. An alternative method is required to organize these results for MFB analysis.

Pressure averaging gives good approximations of the fuel behaviour under the influence of cycle to cycle variation (Swarts et al., 2004). This method averages the pressure values of all cycles obtained from one operating condition. A single pressure trace within the range of data that is closest to the averaged pressure is then taken to represent the characteristic behaviour of the fuel at the particular test condition.

The following graph illustrates the results on the CFR data after pressure averaging, where the thick line is the "characteristic representative" pressure trace.

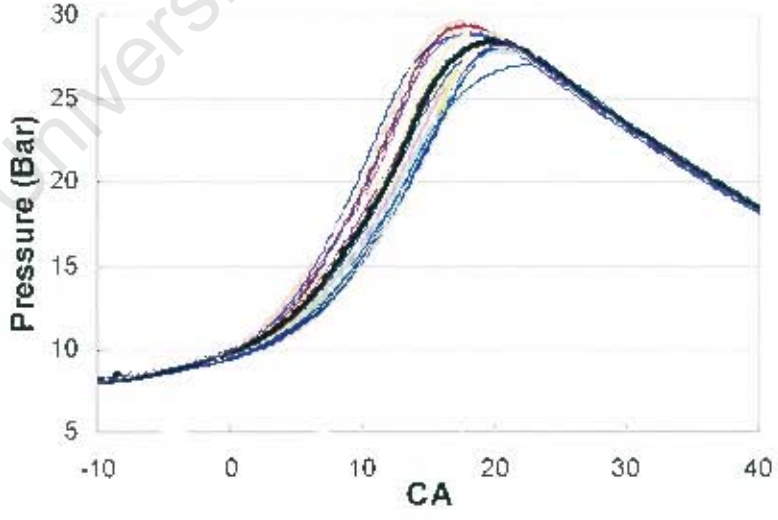

Figure 4-1: Graph illustrating the CFR engine test data with the thick line as the characteristic representative pressure trace

The range of fuels tested in the CFR engine include iso-octane, propane, full boiling range gasoline fuel (synfuel) and a range of fuel blends (see appendix A for blend information). The representative pressure traces for these fuels are illustrated in Figure 4-2 to 4-6, where the legends represent different CR's:

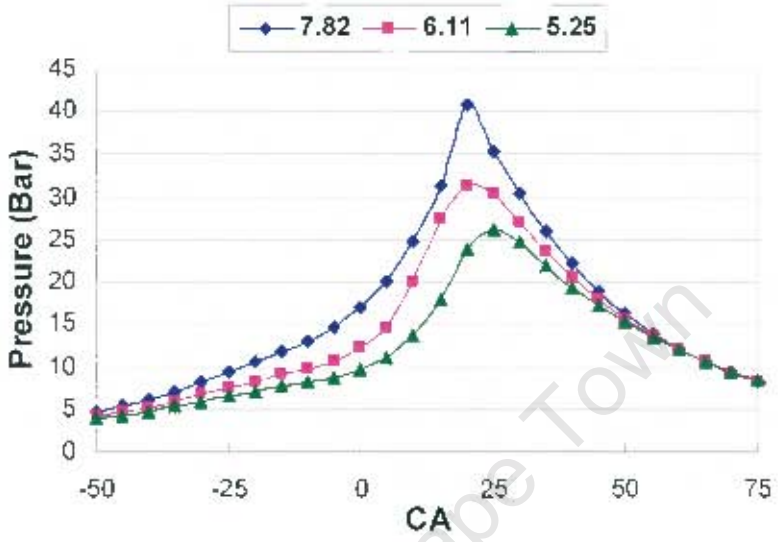

Figure 4-2: Representative pressure data for iso-octane under RON and non-knocking condition and various CR

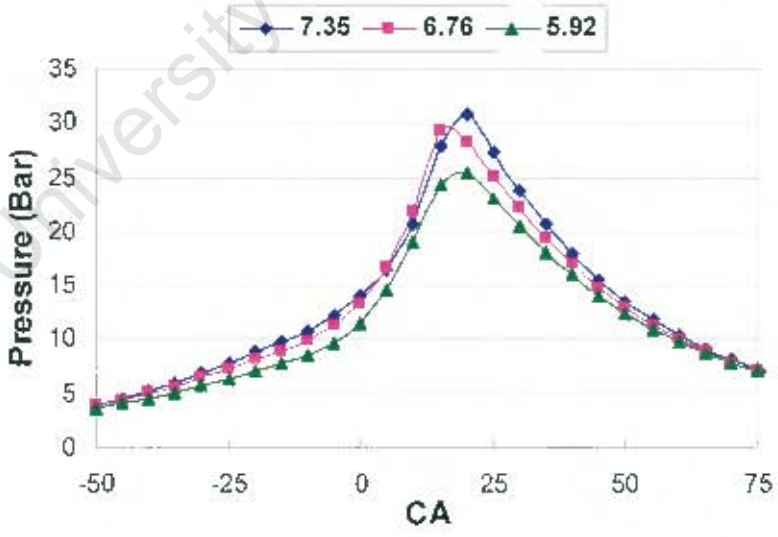

Figure 4-3: Representative pressure data for iso-octane under MON and non-knocking condition and various CR

It is clearly shown in the above graphs of the difference between the RON and MON pressure traces that the spark timing, generally referred as *spark advance* (SA), is different

for RON and MON condition. In the RON condition the SA is fixed at 13° BTDC while in the MON condition the SA is adjusted with different CR to maintain the peak pressure positions at an optimal of 15-20 CAD after TDC.

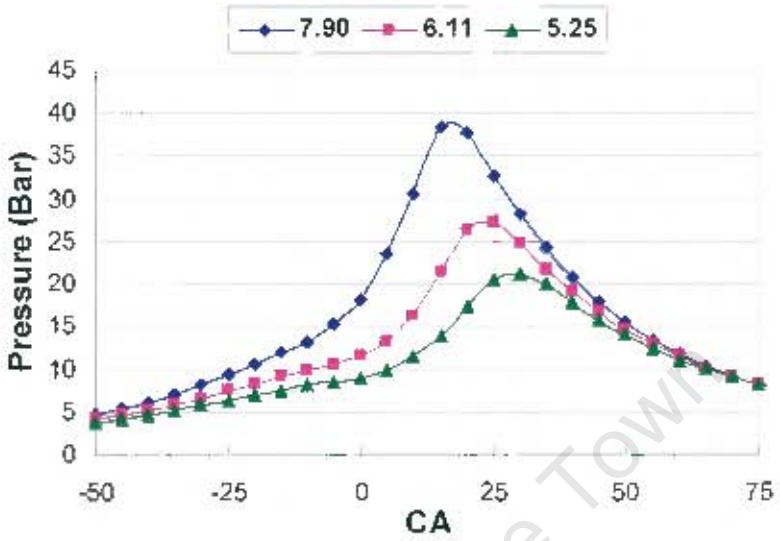

Figure 4-4: Representative pressure data for propane under RON and non-knocking condition and various CR

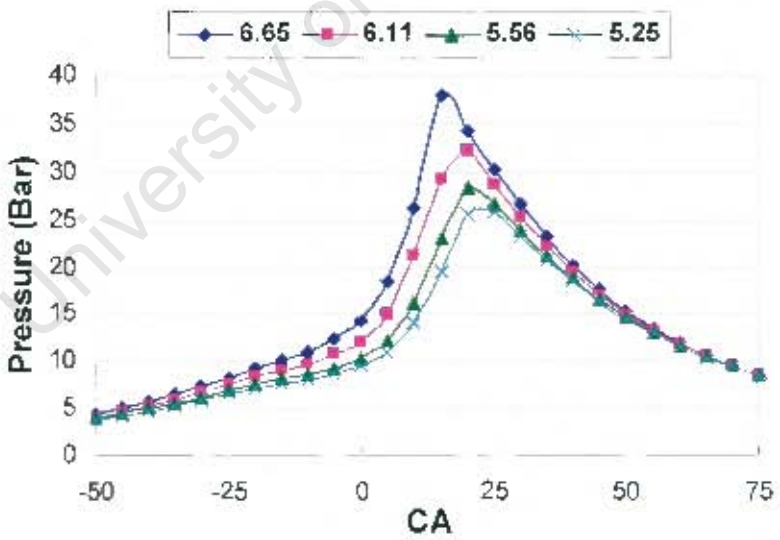

Figure 4-5: Representative pressure data for synfuel under RON and non-knocking condition and various CR with relative air/fuel ratio = 1 (stoichiometric condition)

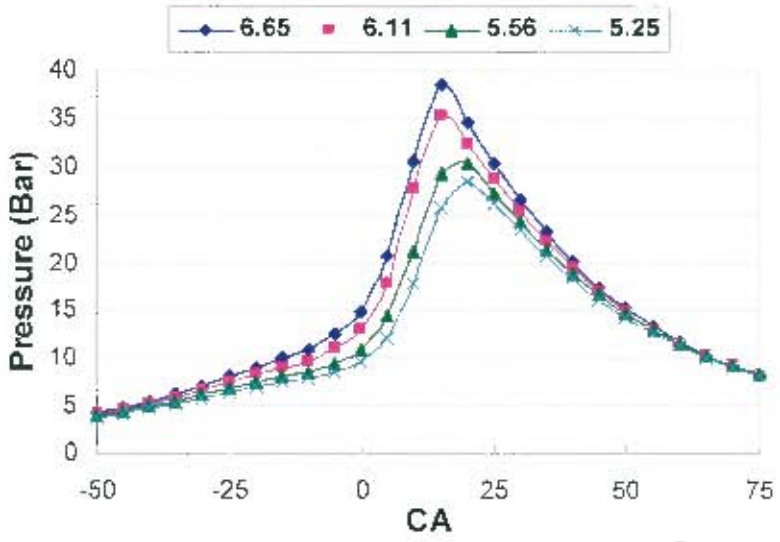

Figure 4-6: Representative pressure data for synfuel under RON and non-knocking condition and various CR with relative air/fuel ratio = 0.9 (fuel rich condition)

Synfuel was tested under RON condition, but under different air-fuel equivalence ratio of λ = 0.9 and 1 (fuel-rich and stoichiometric conditions, respectively). Under the fuel-rich condition it can be observed that the peak pressure is higher than the stoichiometric condition. The reason is a slightly higher energy input into the engine and is consistent with flame speed/ temperature data (Heywood 1988).

4.2 Normal Combustion

4.2.1 Results on CFD analysis

The purpose of the CFD modelling in this application was to analyse the effect of the shrouded valve on the inlet flow development inside the CFR engine prior to combustion. It was especially focused at the area/level in the combustion chamber where the spark plug is fitted. This calculation process begins with the piston moving downwards from TDC, and the inlet valve opens 10° ATDC. The inlet valves closes at 214° ATDC and the piston starts to compress the air inside the cylinder. The calculation stops when the piston reaches TDC again.

Figure 4-7 illustrates the flow velocity development inside the engine. Results are taken from a section of the cylinder at the level where the spark plug is placed. The inlet valve is fitted at the right-hand side of the circular section and the inlet air is guided by the shroud to move in an anti-clockwise manner as indicated. The different colours indicate the levels of velocity magnitude and are not to scale.

In picture (1), the piston moves away from TDC and the inlet valve starts to open. The area with lighter colour shows air entering the cylinder. From picture (2) to (5), the air enters the cylinder as the piston moves down and the cylinder volume increases. When the valve closes at (5) or 214° ATDC, the air forms a helical pattern inside the cylinder and the air velocity is determined by the CR. After IVC, the air is compressed by the ongoing piston and the helical pattern starts to form swirl as the clearance volume becomes smaller and compression also causes air to slow down. Because of the different compression intensity at different CR's, there is only a small (< 10%) velocity different at TDC for high and low CR (7.5 and 5.25 respectively).

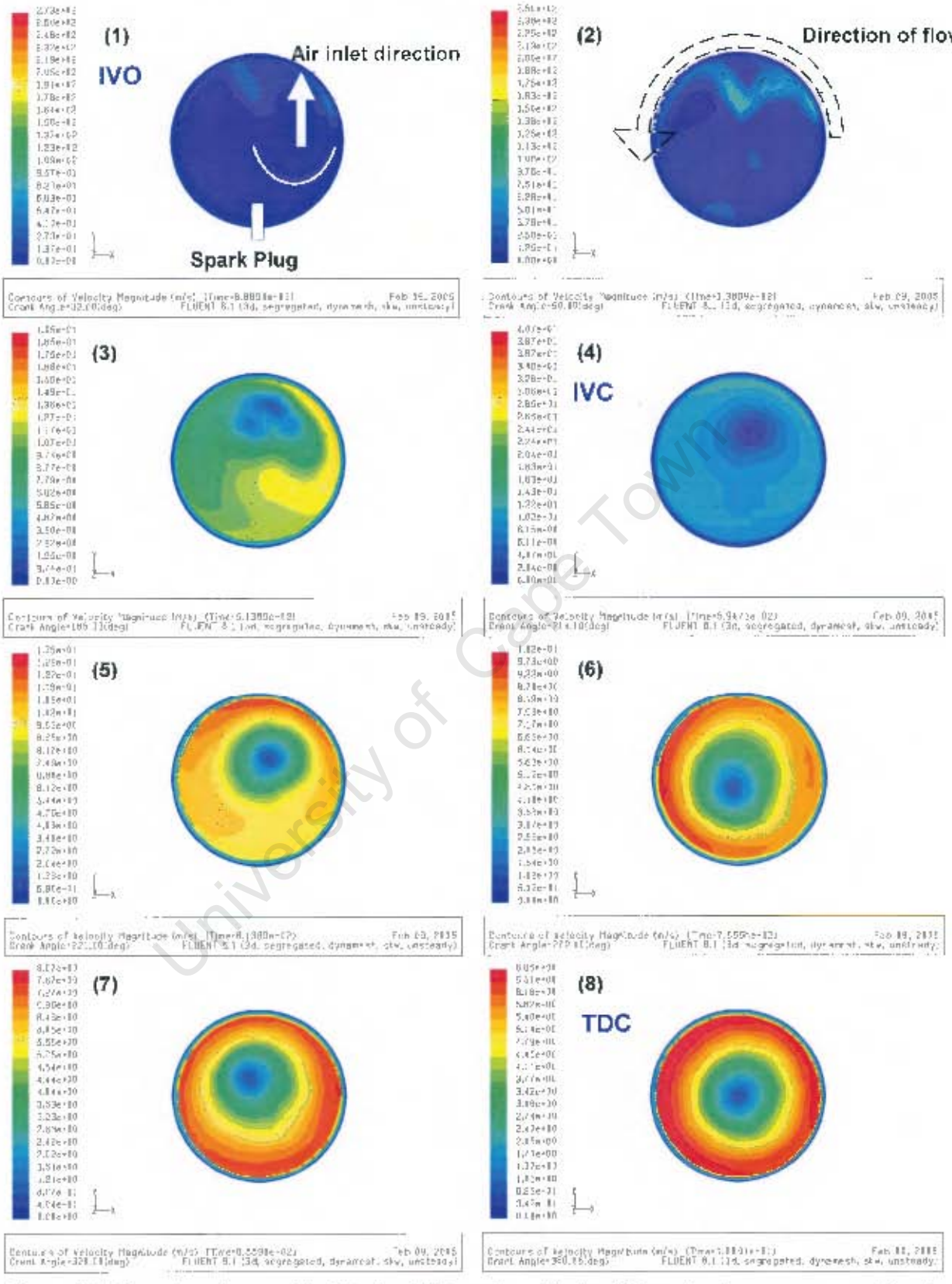

Figure 4-7: Flow development inside the CFR engine with the different colour corresponding to the velocity magnitude on the left hand side

4.2.2 Flame shape assumption

With the results from the CFD analysis and the fact that the CFR engine has a side mounted spark plug; this gave suggestions to two flame shape assumptions:

a) Reversed Cylindrical Flame

This flame shape has a flame front starting from the cylinder wall and propagates toward the centre of the combustion chamber in a circular form. This is one of the extreme cases where by the flame is transported circumferentially around the cylinder by the strong swirl. At the beginning of the combustion the flame front also travels towards the piston and the cylinder head. This allows a three-dimensional growth in the burn volume and after the flame reaches the two boundaries the growth becomes two-dimensional. As the flame propagates the unburned volume decreases in a reduced cylindrical manner.

A picture illustrating this concept is shown in the following Figure, with the sectioned view from the top of the cylinder.

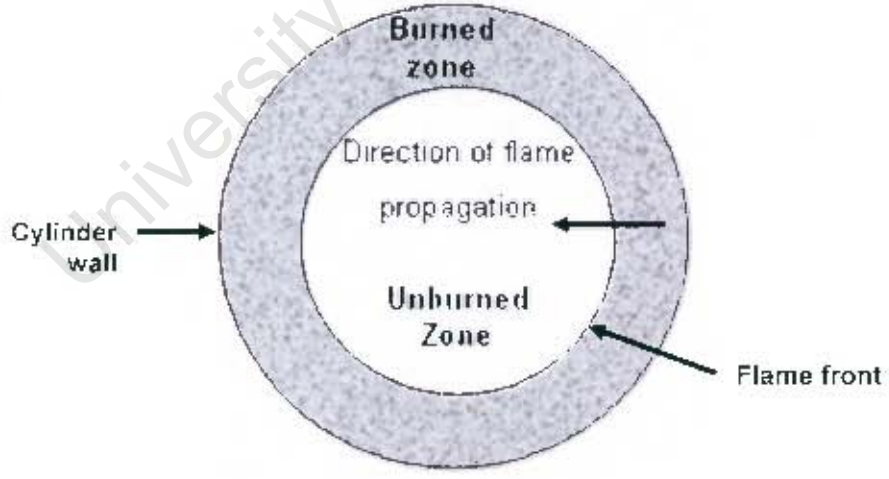

Figure 4-8: Reversed cylindrical flame front concept viewing from the top of the cylinder

b) Side Propagating Flame

This flame shape initiates at one side of the combustion chamber and propagates toward the other side of the chamber. This is the other extreme case whereby the flame is not transported around the cylinder due to quiescent flow. Due to the complex geometry at the

intersection between the flame front and the cylinder wall, a planar flame front is used. As the previous concept, the burn zone volume growth is three-dimensional as the flame propagates toward the piston and the cylinder head.

This concept is illustrated in the following Figure with a sectioned view from the top of the piston.

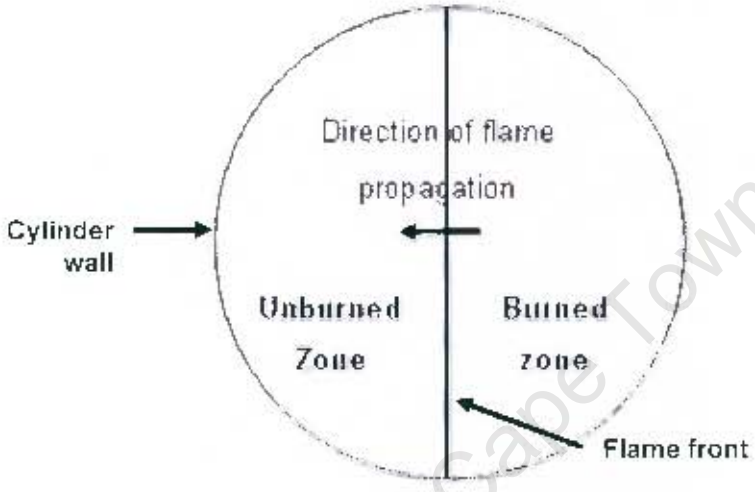

Figure 4-9: Side propagating flame front concept viewing from the top of the cylinder

These two flame shapes were derived from the two extreme cases of operating conditions, where swirling air has very strong or no effect on the flame front formation. In reality, an engine would operate under a wide range of engine speeds and the flame front shape is more likely to be a combination of the two.

4.2.3 Combustion model validation

The two-zone model was used to compare the results obtained under non-knocking RON conditions. Standard test conditions and the burn durations obtained by applying the Rassweiler and Withrow model on the CFR pressure data were used as the primary input for MFB calculation. This is to obtain direct comparisons between the experimental and modelled results. It was noted that for a given fuel, the MFB and burn rate behaves differently at different CR's. At lower CR, it is better described with the reversed cylindrical flame model and at higher CR, the side propagating flame model better describes the MFB behaviour. This is possibly due to the difference in clearance volume caused by different

CR's. From the CFD results it was observed that due to compression, the velocity of the swirling air is significantly reduced. Therefore with the increased level of compression at higher CR, there is more damping effect from the piston to disturbed swirling air and reduce its velocity. It results in the initial flame not being transported around the cylinder fast enough and showed the planar flame behaviour. Difference in CR will also result in pressure and temperature differences, as compression will cause the pressure and temperature to increase. The following Figures will illustrate the comparison between the CFR test results and the modelled results:

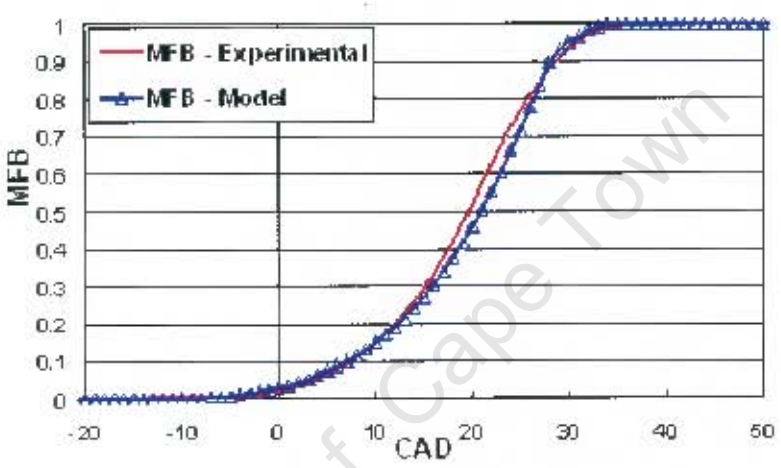

Figure 4-10: MFB comparison using the reversed cylindrical flame model (CR 5.25)

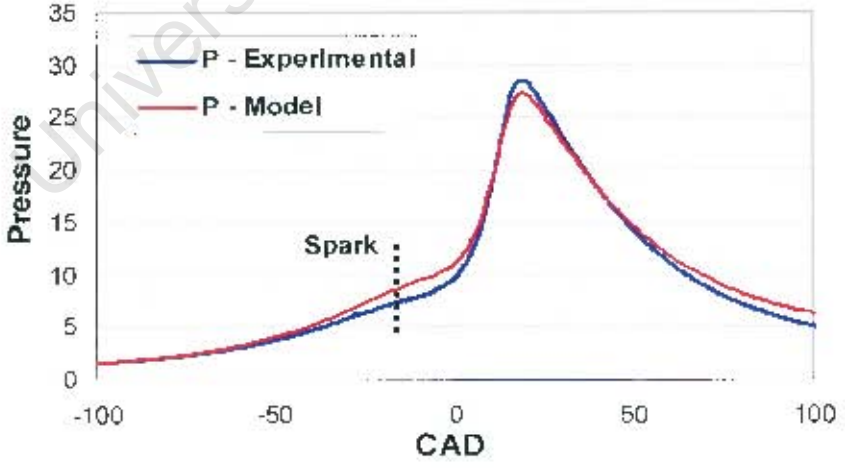

Figure 4-11: Pressure comparison using the reversed cylindrical flame model (CR 5.25)

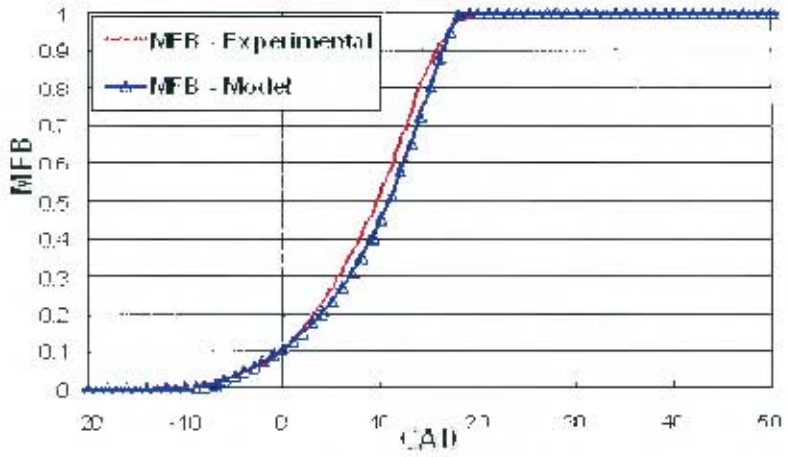

Figure 4-12: MFB comparison using the side propagating flame model (CR 7.902)

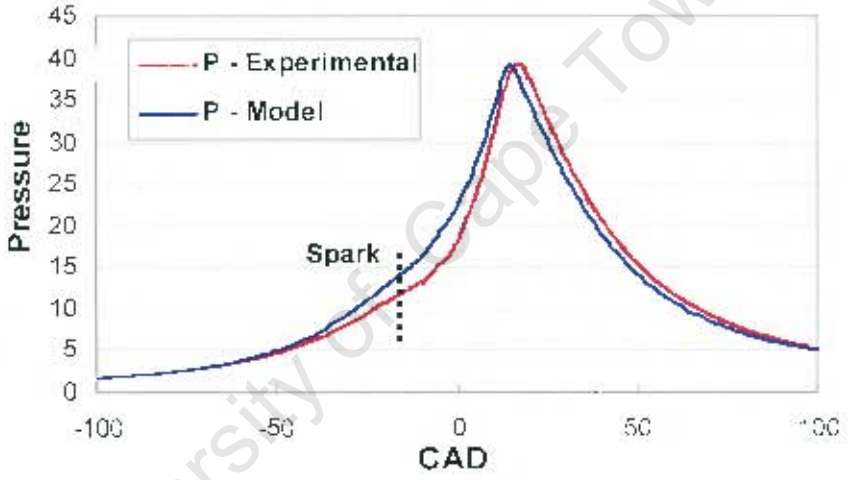

Figure 4-13: Pressure comparison using the side propagating flame model (CR 7.902)

In the pressure comparisons, a small difference in pressure was noted prior to the spark advance. There are some possible explanations for this difference.

- The CR of the CFR engine is controlled by a calibrated gauge, which may contain a small difference between the actual CR and the value on the gauge.
- The flame propagation model assumed fixed mass inside the cylinder during the combustion cycle. For example, no allowance for mass loss through crevice or blow-by
- The model used estimated heat loss correlation derived by Woschni (Woschni, 1967) with the estimation of gas velocity
- The amount and content of the TRG was estimated.

Although there was a small difference in the pressure development, the model still showed good overall correlation. More importantly the MFB behaviour showed a close match between the engine data and the results from the model. Therefore the minor error due to the assumptions made was not considered to be significant.

4.2.4 Turbulent flame factor

Turbulent flame factor (TFF) required for different fuels at different compression ratios were also calculated. TFF was obtained by solving the value of TFF concurrently with the flame propagation model so that the SA and EEOC values in the model match with the ones in the CFR data.

The following graph illustrates the TFF for each fuel as a function of CR:

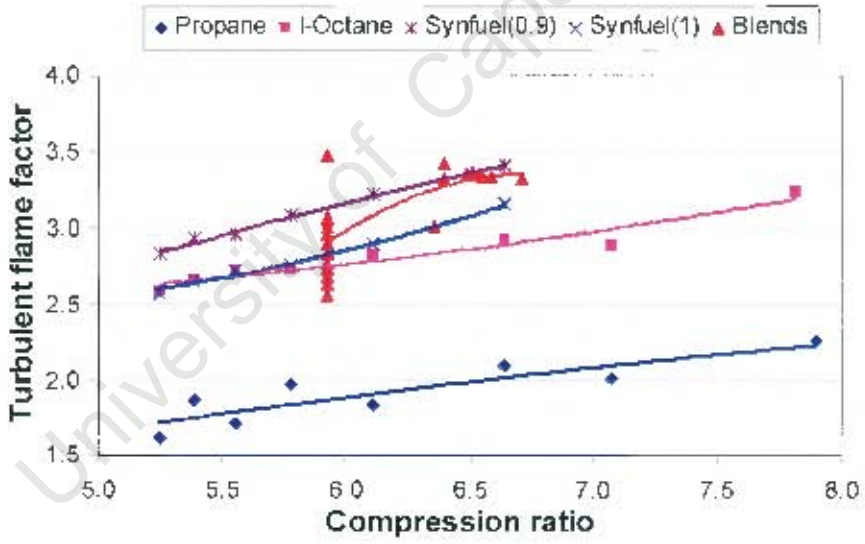

Figure 4-14: Turbulent flame factor as a function of CR for different fuels under RON condition

This graph showed a trend of increasing TFF with respect to increasing CR. Research by Benson et al. (1975) showed a positive trend between the peak temperature during combustion and the TFF. At higher CR, due to higher pre-ignition temperature, the peak temperature during combustion is expected to be higher compared to lower CR combustion. Therefore this trend in the graph correlates well with the results in literature.

A difference can be observed between the magnitudes of TFF for synfuel at the equivalence ratios of 1 and 0.9. At the equivalence ratio of 0.9, the TFF value is higher than the value obtained at stoichiometric condition. Laminar flame speed is a function of air/fuel ratio as can be seen in the literature. Research has shown that the values of laminar flame speed for different fuels reach maximum between stoichiometric and slightly rich air/fuel ratio (Heywood, 1988). The values decrease as the air/fuel ratio becomes lean. Therefore it is reasonable that TFF for synfuel at 0.9 is higher since it has to compensate for the lower laminar flame speed.

It should be noted that although propane also followed the increasing trend with increased compression ratio, there was a distinct difference between propane and the other fuels. The reason for this is because propane is a gaseous fuel and the other fuels are in liquid form. During the intake and compression stroke, evaporation of the liquid fuel results in the change of volumetric efficiency of the intake process and different cylinder condition which will lead to different result.

This model was also used to compare with the results obtained under MON conditions using iso-octane as the test fuel. The comparative results are illustrated in the following Figure.

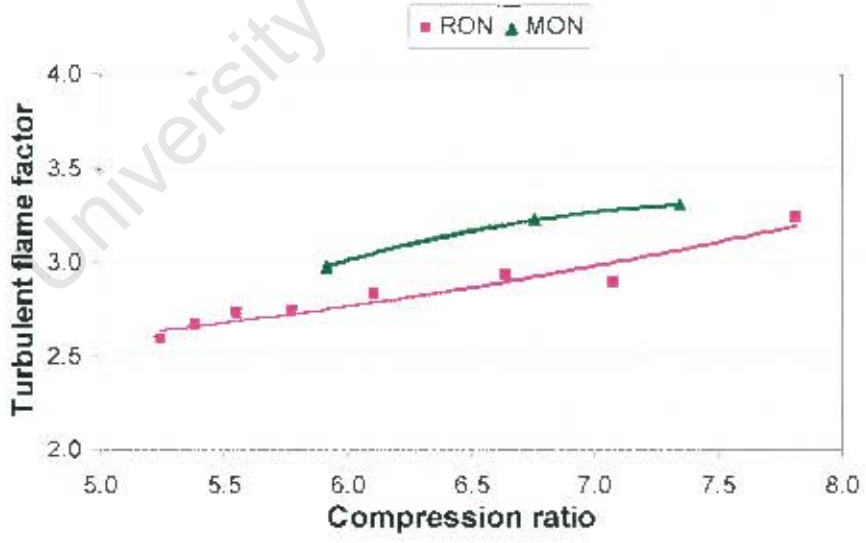

Figure 4-15: Comparison of flame factor for iso-octane under RON and MON condition

Comparison of the RON and MON flame factors only results in a small difference, although the engines runs 50% faster under MON condition (900rpm) compare to RON condition (600rpm). This was because of the laminar flame speed difference between the two test

conditions. The laminar flame speed of fuel is directly proportional to temperature and in-directly proportional to pressure as discussed in Equation (2.4). Under the MON condition the engine operates at higher temperature and lower pressure which results in a significantly increased laminar flame speed comparing to the RON conditions.

The following Figure shows the effect of temperature and pressure on the laminar flame speed, where the y-axis represents the coefficient of the temperature and pressure terms in Equation (2.4).

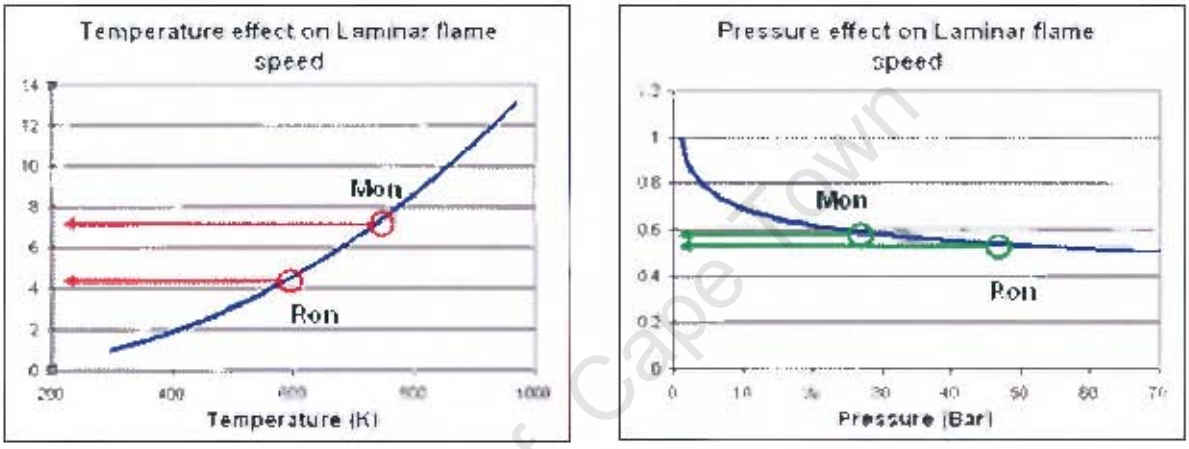

Figure 4-16: Effect of RON and MON operating temperature and pressure on the laminar flame speed with the y-axis representing the coefficient of each term in S_L calculation

It is clear from the graph that under both conditions, the temperature effect overwhelms the pressure effect. Therefore laminar flame speed is higher under MON condition, which effectively lowers the TFF.

4.3 Abnormal Combustion

4.3.1 CFR data under knocking condition

Pressure traces under CFR engine knocking condition were recorded with a range of PRF as the test fue ranging from PRF40 to PRF100. With the use of pressure averaging and the Rassweiler and Withrow method, the MFB comparisons were obtained and some observations were made. As the result of the knocking pressure traces which have linear pressure rise characteristics after the knock-point the MFB curves also contain linear increase regions after the knock-point. The MFB curves for the range of PRF generally behave similar before the knock-point and the rates of increase (slope) after the knock are also very similar. *Mass fraction unburned* (MFU) at the knock-point increases as the ON for PRF decreases and the EEOC also advances towards TDC and results in shorter burn durations since the SA is fixed under RON condition. There observat ons are illustrated in the following Figures:

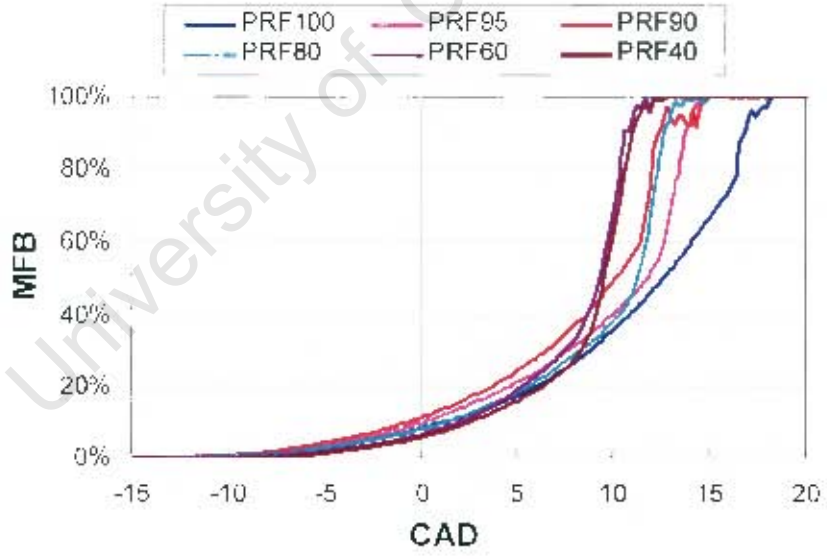

Figure 4-17: MFB curves under knocking conditions a range of PRF

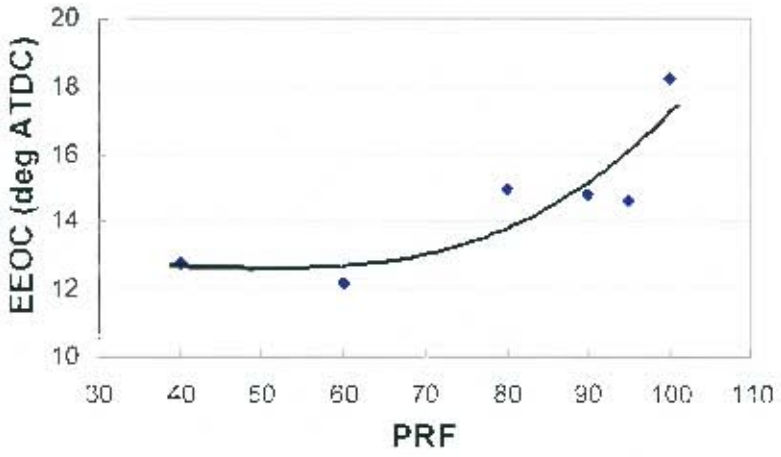

Figure 4-18: Observed EEOC for different PRF under RON condition

4.3.2 Results on the three-zone combustion model

The three-zone model is used to determine the possible effect of the TBL on the auto-ignition behaviour observed in the CFR engine. The main focus was to explore possible relationships between MFU within the TBL and MFU at the knock-point under knocking operation. It was therefore required to compare the calculated results with the experimental data. The model has been programmed to terminate the calculation process once the flame front reaches the TBL, which is when the volume of the unburned gas outside the TBL becomes 0. This was done to ensure that only the combustion due to flame propagation was considered. Combustion after the knock-point is the auto-ignition of the fuel that does not involve flame propagation, which can be observed from the sudden change of combustion rate (refer to appendix C). It was therefore not included into the model.

With the three-zone model including the TBL development, it was observed that the thickness of the TBL decreases and reaches minimum as the piston approaches TDC and increases as the piston moves away from TDC. The following Figure illustrates a typical example of the TBL development as a function of CAD for two different CR's. It can be seen that varying the CR only resulted in a small difference in TBL thickness and TBL development trend was not affected.

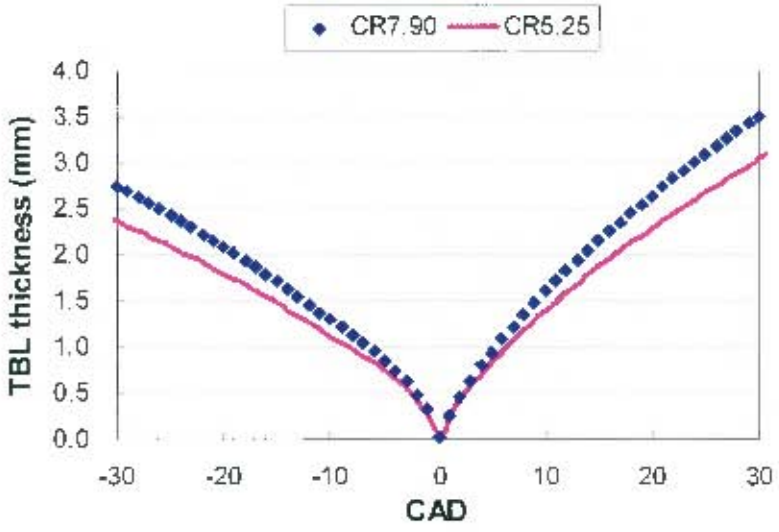

Figure 4-19: Typical examples of TBL thickness development including effect on changing CR

The following graph illustrates the mass distribution in the three-zone model during the three-zone calculation using PRF40, and the mass distribution changes due to combustion and the TBL development. It can also be observed that the calculation ends when the volume of the unburned zone becomes 0 or when the burned zone reaches the TBL.

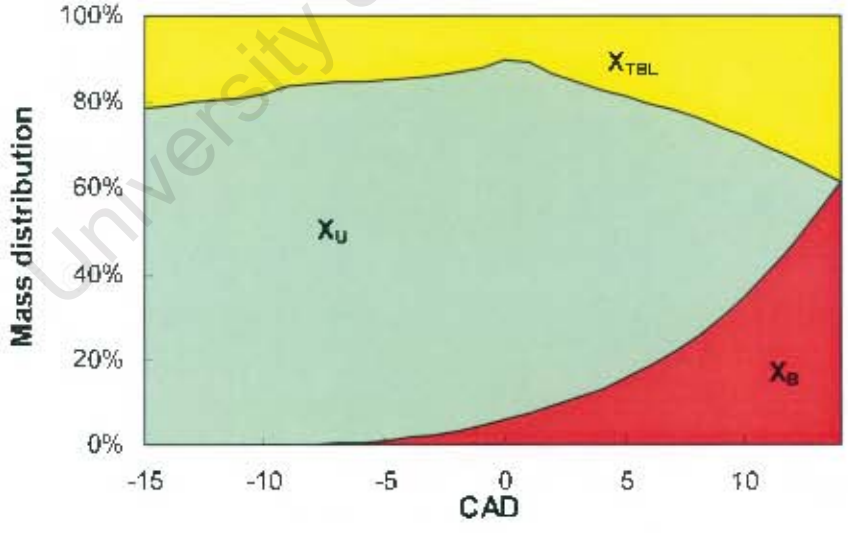

Figure 4-20: Mass distribution within the three zones during combustion for PRF40

The calculated MFB from the three-zone model was then compared with the knocking data from the CFR engine. The comparison is shown in the following Figure:

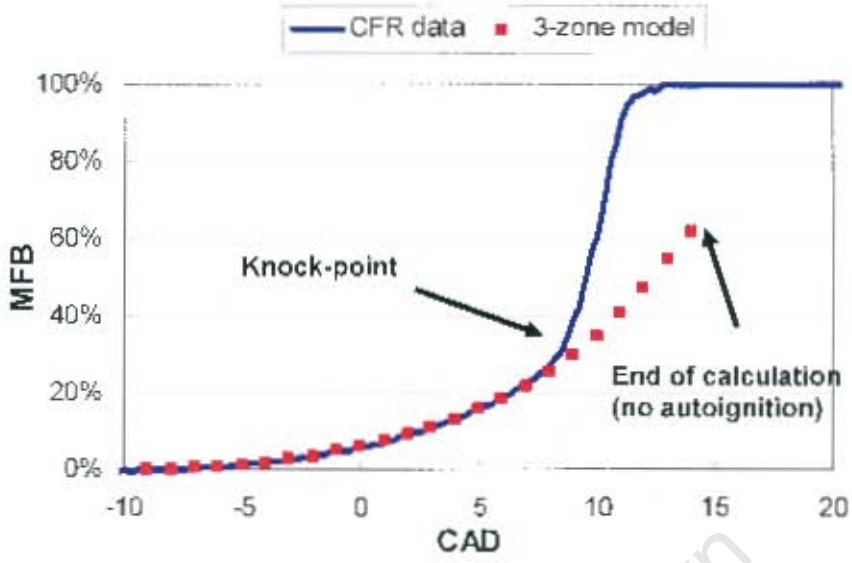

Figure 4-21: Comparison of engine data and three-zone model result using PRF40

It was noted that there was a difference between the experimental knock-point and the end of calculation, taken as the instant when the X_B reaches X_{TBL}. The same trend was observed in the comparisons of the other PRF data and MFB results. The following Figure shows the overall comparison of MFU at the knock-point between the CFR data and the end-of-calculation point of the three-zone model.

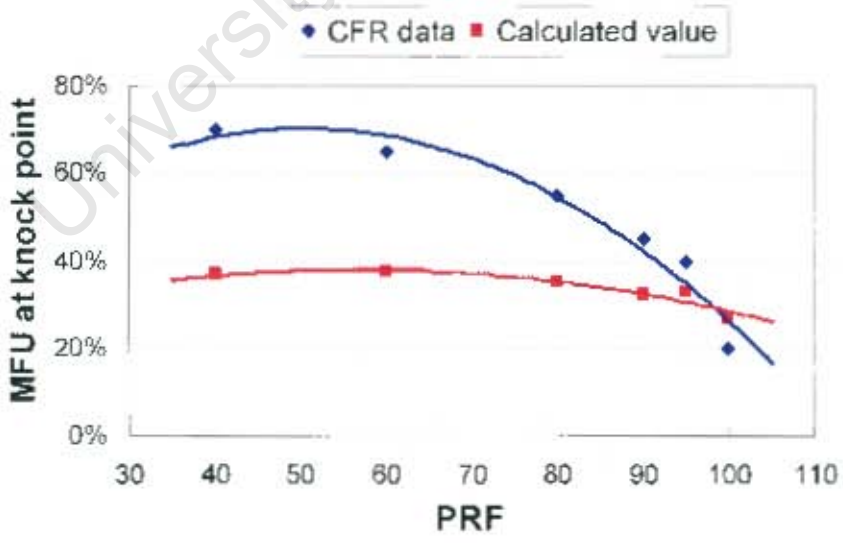

Figure 4-22: Comparison of MFU at knock-point between the CFR data and the end-of-calculation point of the three-zone model

From the comparison it can be seen that the results did not show good correlations. This difference in the unburned mass fractions is caused by the nature of the TBL thickness development. The TBL thickness showed a decreasing trend towards the TDC, which was shown in Figure 4-19. However the MFU at the knock-point in the CFR data showed a completely opposite trend of increasing towards the TDC. The TBL thickness is directly proportional to the TBL volume, which governs the amount of the trapped mass within the TBL. Therefore it is reasonable to use it as an indication of the amount of unburned mass within the TBL at the different stages of the combustion, more specifically, the knock-point. The following graph illustrates the TBL development, as well as indicating the regions where the MFU at knock-point from the CFR data would be expected to fall under.

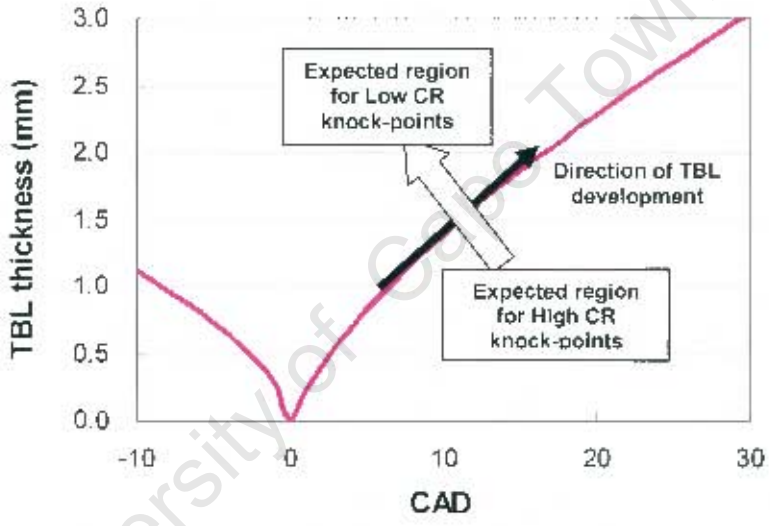

Figure 4-23: Illustrative graph showing the TBL thickness development and the expected region for MFU at knock-point from the CFR data

At higher CR, the positions of the knock-points tend to be further away from the TDC and the MFU also tends to be less, which would correlate to a thinner TBL. Similarly, at lower CR, a thicker TBL is required with the MFU at the knock-point.

4.3.3 Discussion on the three-zone combustion model results

This result showed that TBL does not give consistent explanation for the knock behaviour inside the CFR engine. This led the CFR knock phenomenon to relate with the HCCI combustion behaviour that was pointed out in the literature. It was also pointed out that in the L-head engine similar knock pressure traces were observed. The common feature between the CFR and the L-engine is that they both have side mounted spark plugs, resulting in a longer flame path. This will also lead to a different burned/unburned mixture spread during combustion when compared with commercial SI engines which have spark plug mounted near the centre of the cylinder.

The following diagram will illustrate the effect of the side mount and centre mounted spark plug on flame development.

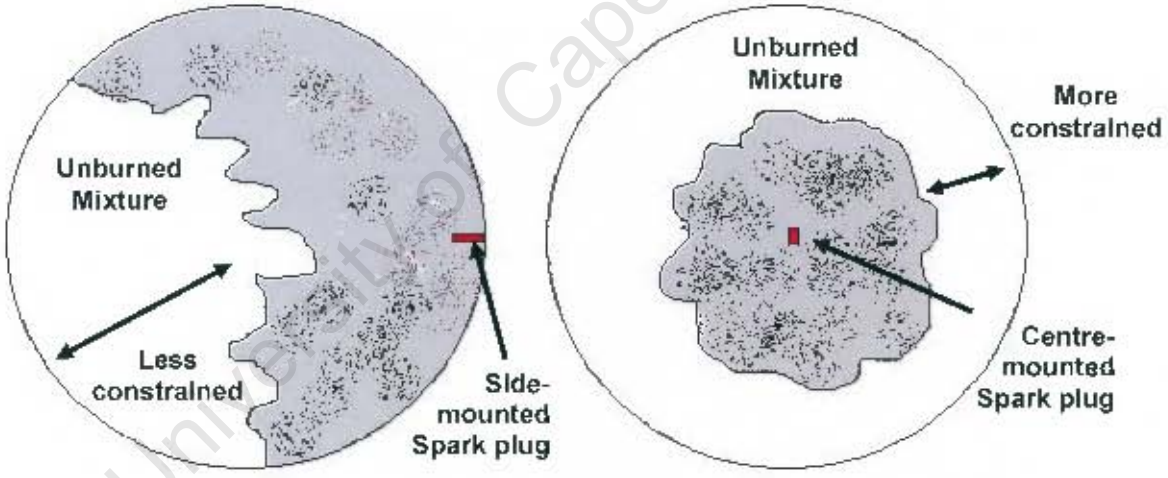

Figure 4-24: Illustrative diagram showing the effect of the spark plug position on flame front development

It can be noted that a side mounted spark plug produces a more localised unburned mixture spread and the mixture is less constrained by the burned gas and the cylinder wall. The centre-mounted spark plug produces a more widely distributed unburned mixture spread and it results in the local unburned mixture being more constrained. Furthermore, commercial SI engines have relative higher CR compare to the L-head and CFR engines and there is less clearance volume. Research by Fitton (1995) showed that if a gas auto-ignites in a more constrained area, it will have a more significant effect on the pressure oscillation and increase possibility to cause engine damages.

This reasonably explained the knock phenomenon inside the CFR engine, that a larger volume is formed due to the result of the flame development. Unburned mixture within this volume is compressed by the piston and the burned gas and then auto-ignites in a HCCI manner. Because of the less constrained area, there are weaker pressure oscillations from the auto-ignition of the fuels.

5. Conclusions and Recommendations

Based on the foregoing information and results, the following conclusions were drawn:

- Combustion model used in conjunction with a two-zone engine model was capable of simulating the combustion event with the flame propagation concept. This model was robust and stable for a variety of fuels, test conditions and engine speeds. Both side propagating and reversed cylindrical flame shape assumptions proved to be good approximations of the actual combustion event in the CFR engine.

- CFD simulation showed the effect of the shrouded inlet valve on the in-cylinder flow development in the CFR engine. The shrouded valve resulted in an increased in-cylinder air velocity and strong swirling motion prior to combustion.

- Comparisons of TFF with different fuels indicated clear difference between liquid and gaseous fuels in which in-cylinder evaporation affects the engine volumetric efficiency. Despite the 50% faster engine speed for the MON test condition, the temperature was shown to have a strong influence on the laminar flame speed. Therefore there was no distinct difference in the TFF value between RON and MON condition although the engine speed difference is significant.

- Through the application of the three-zone engine model, no direct relation was found between the trapped mass within TBL and the unburned mass at the knock-point. It was shown that the presence of the TBL was not singularly responsible for the knock-point on the thermal inhomogeneity.

- The HCCI-like combustion of the end-gas observed after the knock-point in the CFR engine was likely due to inhomogeneity in the end-gas. This is generally referred to as developing detonation. Side mounted spark-plug and the large clearance volume associated with the low CR would likely to cause the localised unburned gas mixture distribution and inhomogeneity within the end-gas.

- Flame propagation prior to the knock-point is similar for all the PRF. This was observed from the conic-cylindrical flame propagation model presented in appendix C.

On the basis of the above results and conclusions, the following recommendations can be made

- The accuracy of the existing model can be improved by reducing the time step sizes and using more calculation constraints. Flame shapes with complex geometries can be considered if possible.

- Predictive auto-ignition model can be included in the flame propagation model for more detailed analysis to allow for the pressure development after the knock-point.

- Perform more engine tests on different fuels for more information on fuel combustion behaviour, especially gaseous fuels. Further tests should be performed under both knocking and non-knocking condition under MON setup.

- Develop a detailed CFD model of the CFR engine for a better simulation of the combustion event. The CFD model should cater for fuel droplet evaporation, mixing and combustion. This will allow for proper selection of the flame shape between the two extreme cases presented in this report.

6. References

Aceves et al. (2001), 'HCCI Combustion: Analysis and Experiments', SAE paper 2001-01-2077

ASTM manual (2001a), Standard Test Method for Research Octane Number of a Spark-Ignition Engine Fuel, D2699-01a

ASTM manual (2001b), Standard Test Method for Motor Octane Number of a Spark-Ignition Engine Fuel, D2700-01a

Arrigoni et al. (1974), 'High Speed Knock in SI Engines', SAE paper 741056

Benson et al. (1975), 'A Simulation Model Including Intake and Exhaust Systems for a Single Cylinder Four-Stroke Cycle Spark Ignition Engine', Int. J. mech. Sci. Pergamon Press, Vol 17

Bradley et al. (2003), 'Turbulent Burning Velocity, Burned Gas Distribution, and Associated Flame Surface Definition', Combustion and Flame 113 (2003) 415-430

Broeze, J.J. (Unknown), *Combustion in Piston Engines*, De Technische Uitgeverij H. Stam N.V., Haarlem

Brunt, M.F. and Emtage, A.L. (1997), 'Evaluation of Burn Rate Routines and Analysis Errors', SAE paper 970037

Cengel, Y.A. and Boles, M.A. (2002), *Thermodynamics: an Engineering Approach*, 4th edition, New York, McGraw-Hill Book Company

Cox, R. (2004), *CFD based engine model,* unpublished work, University of Cape Town

Cox, R. (2005), Personal communication

Fan, L. and Reitz, R.D. (2000), 'Development of an Ignition and Combustion Model for Spark Ignition Engines', SAE paper 2000-01-2809

Fitton, J.C. (1995), *Knock-Erosion Damage in Spark Ignition Engines*, M.Sc. thesis, University of Cape Town

Flowers et al. (2000), 'HCCI in a CFR Engine: Experiments and Detailed Kinetic Modelling', SAE paper 2000-01-0328

Fluent (1998), [Computer software], Release 6.1.22, Fluent Inc.

Fujimoto et al. (2002), 'Effect of combustion chamber shape on tumble flow, squish-generated flow and burn rate', JSAE paper 20024247

Hacohen et al. (1994), 'Flame Speeds in a Spark Ignition Engine', SAE paper 942050

Hajireza et al. (1999), 'A Three-Zone Model for Investigation of Gas Behaviour in the Combustion Chamber of SI Engines in Relation to Knock', SAE paper 1999-01-0219

Heywood, J.B. (1988) *Internal Combustion Engine Fundamentals*, New York, McGraw-Hill Book Company

Keck, J.C. (1982) 'Turbulent Flame Structure and Speed in Spark-Ignition Engine', Proceeding of the Nineteenth International Symposium on Combustion, The Combustion Institute

Konig, G. and Sheppard, C.G.W. (1990), 'End Gas Autoignition and Knock in a Spark Ignition Engine', SAE paper 902135

Kuehl, D.K., (1962), *Eighth Symp. (Int.) on Combustion*

Kumar, S. and Watson, H.C. (1988), 'Flame Propagation in a High-speed Variable Swirl Spark Ignition Engine', Journal of the Institute of Mechanical Engineers C61

Lee et al. (1998), 'Flame Speed Measurements and Prediction of Propane, Butane and Autogas at High Pressures', SAE paper 982448

Lee, T.W. and Lee, S. J. (2003), 'Direct Comparison of Turbulent Burning Velocity and Flame Surface Properties in Turbulent Premixed Flames', Combustion and Flame 132 (2003) 492-502

Lyford-Pike, E.J. and Heywood, J.B. (1984), 'Thermal Boundary Layer Thickness in the Cylinder of a Spark-Ignition Engine', Int. J. Heat Mass Transfer, Vol. 27, No. 10

Maly, R. and Ziegler, G. (1982), 'Thermal Combustion Modelling – Theoretical and Experimental Investigation of the Knocking Process', SAE paper 820759

Oppenheim, A.K. and Kuhl, A.L. (1998), 'Life of Fuel in Engine Cylinder', SAE paper 980780

Pan, J. and Sheppard, C.G.W. (1994), 'A Theoretical and Experimental Study of the Modes of End Gas Autoignition Leading to Knock in S.I. Engine', SAE paper 942060

Rassweiler, G.M. and Withrow, L. (1938), 'Motion Pictures of Engine Flames Correlated with Pressure Cards', SAE transactions volume 42

Ryan, T.W. and Lestz, S.S. (1980), 'The Laminar Burning Velocity of Isooctane, N-Heptane, Methanol, Methane, and Propane at Elevated Temperature and Pressures in the Presence of a Diluent', SAE paper 800103

Sonntag et al. (1998), *Fundamentals of Thermodynamics*, 5th edition, New York, John Wiley & Sons Inc.

Swarts, A. (2006), Unpublished PhD. Thesis, due to be published in 2006, University of Cape Town

Swarts et al. (2004), 'Standard Knock Intensity Revisited: Atypical Burn Rate Characteristic Identified in the CFR Octane Rating Engine', SAE paper 2004-01-1850

Swarts et al. (2005), 'A Further Study of Inconsistencies between Autoignition and Knock Intensity in the CFR Octane Rating Engine', SAE paper 2005-01-2081

Taylor, C.F. and Taylor, E.S. (1962), *The Internal Combustion Engine*, 2nd Edition, Pennsylvania, International Textbook Company

Versteeg et al. (1995), *Introduction to Computational Fluid Dynamics: the finite volume method*, New York, Longman Scientific & Technical Wiley

Woschni, G. (1967), 'Universally Applicable Equation for the Instantaneous Heat Transfer Coefficient in the Internal Combustion Engines', SAE paper 670931, SAE Trans. Vol.76

APPENDICES

Appendix A: Blend Information

Appendix B: Flow Diagram of the Flame Propagation model

Appendix C: Conic-Cylindrical Shaped Flame Propagation Model

A. Blend Information

The following table shows the components of the blends that were used for comparison.

Table A-1: Information on the blends used for comparison

Blend No.	RON	% Etoh	% Prop	% Hex	% Tol	% Hep	% Oct
1	100.4	10	0	0	40	12.5	37.5
2	99.7	0	10	0	40	12.5	37.5
3	87.5	0	0	30	20	12.5	37.5
5	90	10	0	30	10	12.5	37.5
6	95.6	0	0	10	40	12.5	37.5
7	88.7	5	0	30	15	12.5	37.5
8	94.6	0	10	15	25	12.5	37.5
9	87.9	0	5	30	15	12.5	37.5
10	96.1	10	0	15	25	12.5	37.5
11	91.2	0	0	20	30	12.5	37.5
13	88.7	0	10	30	10	12.5	37.5
17	92	2	0	19	29	12.5	37.5
18	91.4	0	2	19	29	12.5	37.5

Etoh - Ethanol
Prop - Propanol
Hex - Hexene
Tol - Toluene
Hep - N-heptane
Oct - I-octane

B. Flow Diagram of the Flame Propagation Model

The two-zone flame propagation starts the calculation at IVC and ends at EVO. Firstly the engine properties and operating conditions are set, as well as the fuel selection. Initial condition is calculated and the TFF is solved according to the input spark timing and the EEOC value. Before the spark advance, there is only the unburned zone and performing energy balance will solve for pressure. After the spark initiates, the volume of the burned zone can be calculated from the turbulent flame speed. Energy balance equation and equilibrium can be used to solve pressure and the burned zone temperature. The calculation is stopped once EVO is reached.

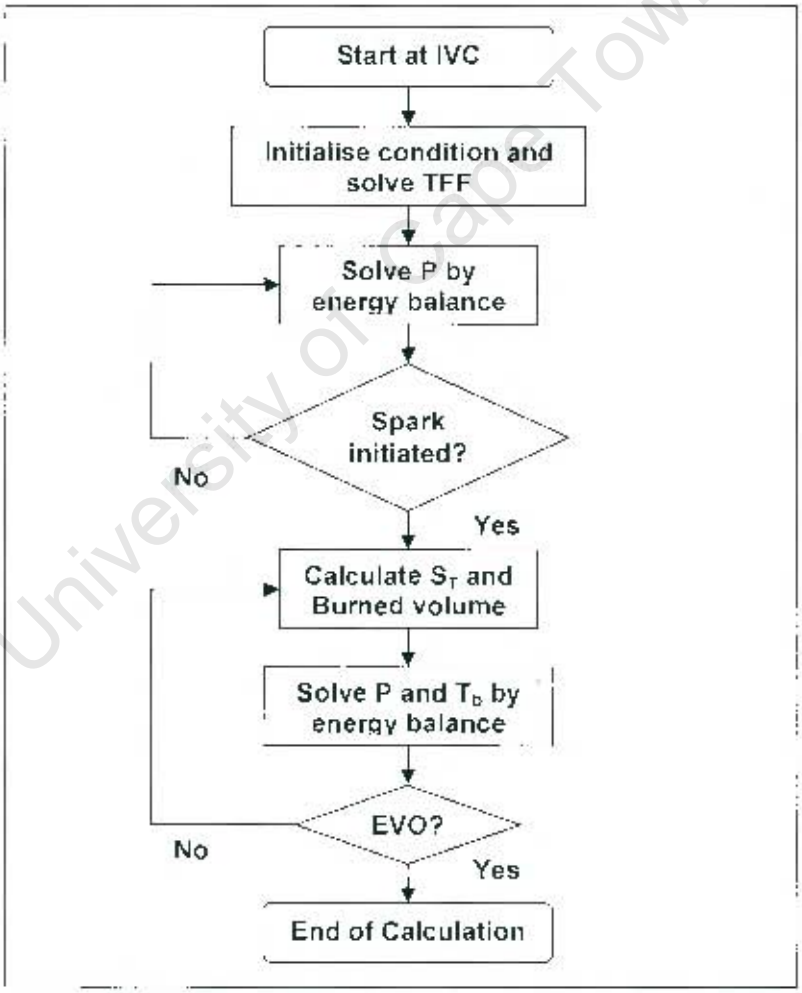

Figure B-1: Flow diagram for the flame propagation model

The calculation process for the three zone model follows the same process of for the two-zone model, except that the calculation is stopped once the flame front reaches the TBL.

C. Conic-Cylindrical Shaped Flame Propagation Model

C.1 Model Description

An alternative approach was found useful to simulate the MFB behaviour, especially for the knocking conditions. This is done by creating a two-zone model that is similar to the one developed for this thesis. However, combustion is not bounded by the engine cylinder and the piston, and a separate volume is created for the combustion event. This combustion volume is a combination of two conic-cylindrical shaped volumes. The main reason and the advantage of this two-volume combination concept was that the start and end of the combustion event can be easily simulated by changing the parameters of the two volumes. The following figure shows the schematic diagram of the model:

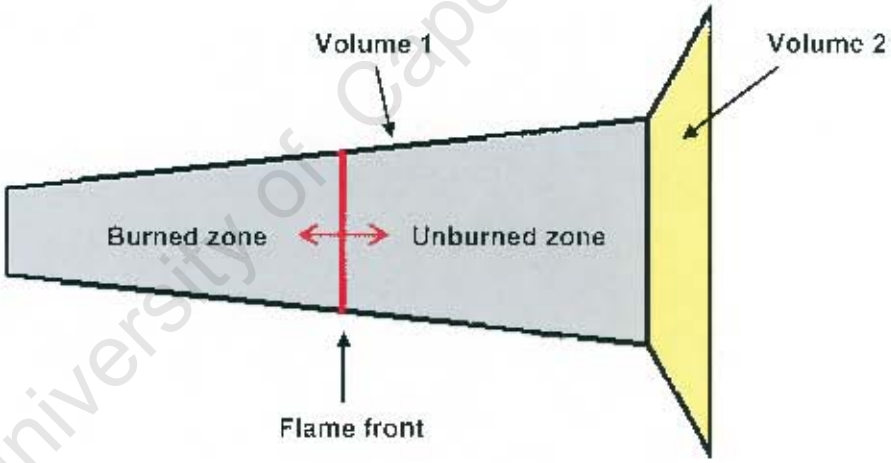

Figure C-1: Schematic diagram of the conic-cylindrical shaped model under knocking condition

For knocking conditions, the end of combustion is characterised by the sudden pressure rise, which is the result of autoignition in the end-gas and a sudden change in the rate of combustion. In non-knocking conditions, the rate of combustion slows down as it reaches the end of combustion due to quenching of the flame. To cater for this difference in the end of combustion behaviours, the direction of volume 2 (direction of the cone) can be changed to shift between knocking and non-knocking conditions. This is illustrated in the following figure:

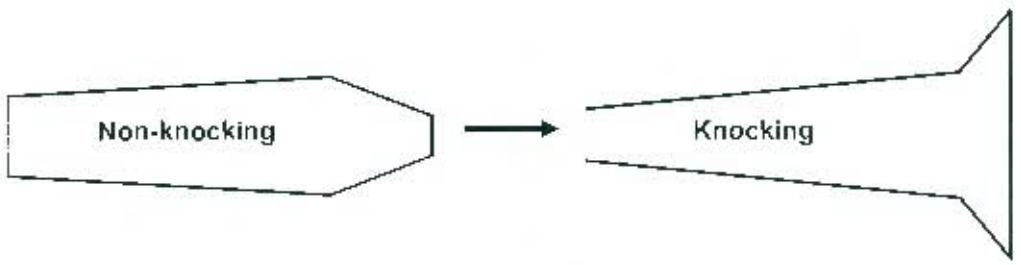

Figure C-2: Comparison of the model under knocking and non-knocking conditions

C.2 Results

There are 5 variables that determine the shape of the model, which determine the MFB characteristic of the model, which are:

- Smaller diameter of volume 1
- Slope of volume 1
- Slope of volume 2
- Total length of the model
- Length ratio between volume 1 and 2

For the ease of comparison between different fuels, it is feasible to minimise the number of variables by assigning fixed values for the variables. When fitting the model to a series of engine data with similar fuel characteristics such of PRF, the total length of both conic-cylinders was fixed to a constant value of 2/3 of the circumference of the cylinder. The smaller diameter of volume was also kept to be as similar as possible.

The following figures showed the results of the model when fitted against the CFR knocking data under RON condition. The model used to fit a low octane fuel (PRF40) and a higher octane fuel (PRF100) to test its ability to simulate MFB behaviours. Comparison of the shapes of the model that best describe a range of PRF fuels was also illustrated

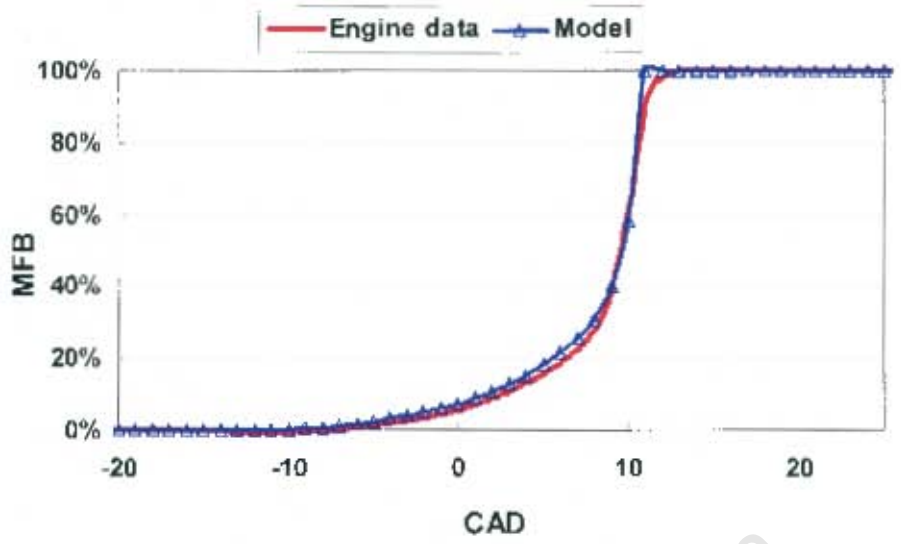

Figure C-3: Conic-cylindrical shaped model fitted to the PRF40 MFB curve under knocking condition

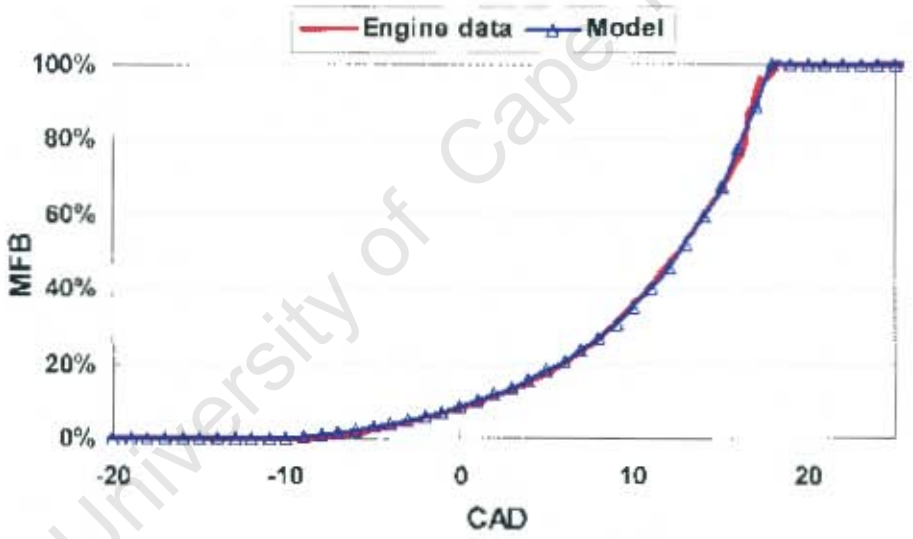

Figure C-4: Conic-cylindrical shaped model fitted to the PRF100 MFB curve under knocking condition

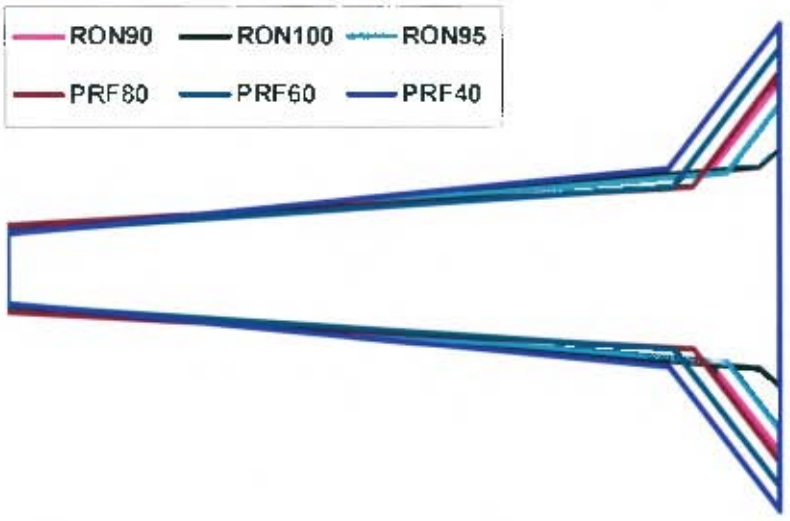

Figure C-5: Comparison of the shape that best describe the MFB behaviour for a range of PRF

It can be observed that the slopes of volume 1 are similar of all the PRF fuel concerned, as well as the slopes for volume 2. There is a sudden change in slopes when moving from volume 1 to volume 2 due the end-gas autoignition, which results in increased combustion rate. Ratio of volume 1 to volume 2 increases as the ON of the PRF increases, indicating a reduced trend of MFU at knock-point with increasing ON. These observations correlate well with behaviours seen in figure 4-17, Chapter 4.

C.3 Conclusions

This two-zone model concept is capable of producing MFB that fits the engine data with no limitation of fuel type or operating conditions. It can also produce comparisons of the fuel combustion characteristic in an easy-to-understand, graphical manner. Therefore the possibilities with this model should be further explored.